Sickle cell disease biochip: a functional red blood cell adhesion assay for monitoring sickle cell disease

YUNUS ALAPAN, CEONNE KIM, ANIMA ADHIKARI, KAYLA E. GRAY, EVREN GURKAN-CAVUSOGLU, JANE A. LITTLE, and UMUT A. GURKAN

CLEVELAND, OHIO, USA

Sickle cell disease (SCD) afflicts millions of people worldwide and is associated with considerable morbidity and mortality. Chronic and acute vaso-occlusion are the clinical hallmarks of SCD and can result in pain crisis, widespread organ damage, and early movtality. Even though the molecular underpinnings of SCD were identified more than 60 years ago, there are no molecular or biophysical markers of disease severity that are feasibly measured in the clinic. Abnormal cellular adhesion to vascular endothelium is at the root of vaso-occlusion. However, cellular adhesion is not currently evaluated clinically. Here, we present a clinically applicable microfluidic device (SCD biochip) that allows serial quantitative evaluation of red blood cell (RBC) adhesion to endothelium-associated protein-immobilized microchannels, in a closed and preprocessing-free system. With the SCD biochip, we have analyzed blood samples from more than 100 subjects and have shown associations between the measured RBC adhesion to endothelium-associated proteins (fibronectin and laminin) and individual RBC characteristics, including hemoglobin content, fetal hemoglobin concentration, plasma lactate dehydrogenase level, and reticulocyte count. The SCD biochip is a functional adhesion assay, reflecting quantitative evaluation of RBC adhesion, which could be used at baseline, during crises, relative to various long-term complications, and before and after therapeutic interventions. (Translational Research 2016;173:74–91)

Abbreviations: CBC = complete blood count; EDTA = ethylenediaminetetraacetic acid; FCSB = flow cytometry staining buffer; FN = fibronectin; GMBS = N-g-Maleimidobutyryloxy succini-

From the Case Biomanufacturing and Microfabrication Laboratory, Mechanical and Aerospace Engineering Department, Case Western Reserve University, Cleveland, Ohio, USA; Department of Electrical Engineering & Computer Science, Case Western Reserve University, Cleveland, Ohio, USA; Department of Hematology and Oncology, School of Medicine, Case Western Reserve University, Cleveland, Ohio, USA; Seidman Cancer Center at University Hospitals, Case Medical Center, Cleveland, Ohio, USA; Biomedical Engineering Department, Case Western Reserve University, Cleveland, Ohio, USA; Department of Orthopedics, Case Western Reserve University, Cleveland, Ohio, USA; Advanced Platform Technology Center, Louis Stokes Cleveland Veterans Affairs Medical Center, Cleveland, Ohio, USA.

Umut A. Gurkan, PhD, is an Assistant Professor in Mechanical and Aerospace Engineering Department at Case Western Reserve University. Dr. Gurkan aspires to develop micro/nano technologies for clinical translation to improve patients' lives. His current research focus is on translational technologies for diagnosis, screening, and monitoring of sickle cell disease. Dr. Gurkan is a recipient of 2016 National Science Foundation Faculty Early Career Development Award.

Submitted for publication August 27, 2015; revision submitted March 8, 2016; accepted for publication March 12, 2016.

Reprint requests: Jane A. Little, Associate Professor, Director, Adult Sickle Cell program Co-Program Director, Hematology and Oncology Fellowship Program, Case Western Reserve University, Seidman Cancer Center at University Hospitals, Case Medical Center, 11100 Euclid Ave, Cleveland, OH 44106; e-mail: jane.little@uhhospitals.org or Umut A. Gurkan, Assistant Professor, Case Biomanufacturing and Microfabrication Laboratory, Mechanical and Aerospace Engineering Department, Biomedical Engineering Department, Department of Orthopaedics, Case Western Reserve University, Advanced Platform Technology Center, Louis Stokes Cleveland Veterans Affairs Medical Center, Office: Glennan 616B, 10900 Euclid Ave, Cleveland, OH 44106; e-mail: umut@case.edu.

1931-5244/$ - see front matter

http://dx.doi.org/10.1016/j.trsl.2016.03.008

mide ester; Hb = hemoglobin; LDH = lactate dehydrogenase; LN = laminin; RBC = red blood cell; SCD = sickle cell disease

AT A GLANCE COMMENTARY

Alapan Y, et al.

Background

Abnormal cellular adhesion to endothelium is at the root of vaso-occlusion in sickle cell disease (SCD). However, cellular adhesion is not currently evaluated clinically because these analyses are technically challenging and difficult to reproduce. This has limited the widespread applicability of adhesion assays clinically or as a research tool in SCD.

Translational Significance

We developed a microfluidic system that allows serial quantitative evaluation of red blood cell adhesion to endothelium proteins in a closed and preprocessing-free system. The presented in vitro adhesion assay would enable a comprehensive and integrated evaluation of red blood cell adhesive properties, which could be used at baseline, during crises, and with therapeutic interventions in SCD.

INTRODUCTION

In mammals, the red blood cell (RBC) has uniquely evolved to lose its nucleus and organelles to become remarkably flexible.[1] RBC's adherence to vascular wall and other cells is insignificant,[2] whereas most other cell types depend on adhesive interactions to survive.[3] RBC repeatedly deforms and squeezes through narrow capillaries that can be as small as half of its diameter.[2,4,5] Its characteristic shape and exceptional mechanical deformability are determined by its membrane skeleton, which is located underneath the cell membrane and linked to adhesion receptors on the cell surface.[6-9] RBC's reduced deformability and increased adhesion have been associated with microcirculatory impairment in many diseases, including hemoglobin disorders,[10-14] sepsis,[15,16] malaria,[17-20] lupus,[21,22] heavy metal exposure,[23,24] blood transfusion complications,[25,26] diabetes,[27,28] cancer,[29,30] kidney diseases,[31-35] cardiovascular diseases,[36,37] obesity,[38,39] and neurologic disorders.[40-43] These diseases affect hundreds of millions of people globally with a socioeconomic burden of hundreds of billions of dollars annually.[44-51]

In sickle cell disease (SCD), RBC adhesion has been associated with blood flow blockage,[52,53] disease severity,[10-13] and organ damage.[54] SCD arises from a point mutation in the β-globin gene resulting in production of hemoglobin S (HbS). Intracellular HbS molecules polymerize on deoxygenation, forming long fibers that lead to membrane damage and abnormal cellular stiffness. Membrane damage caused by HbS polymerization increases sickle RBC adhesion to vascular endothelium.[55,56] In addition, increased RBC stiffness impacts blood flow and, with abnormal cellular adhesion, results in blockage of blood vessels (vaso-occlusion).[52,53]

SCD affects millions worldwide[57] and imposes significant physical, emotional, and financial burdens on its sufferers, their families and communities. Chronic and acute vaso-occlusion are the clinical hallmarks of SCD and can result in painful crises, cumulative organ damage, and early mortality.[56] SCD can cost >$8 million per patient over a 50-year life span (in the United States).[58] Even though abnormal RBC adhesion is the centerpiece of vaso-occlusion and vascular damage in SCD, there is no clinically relevant tool or method to evaluate cellular adhesion as a clinical biomarker for disease severity. Lack of such clinically applicable assays has slowed the development of new pharmaceutical and therapeutic approaches because there is no in vitro test for measuring the effects of these interventions on RBC adhesion. To address this clinically unmet need, we developed a versatile microfluidic platform for evaluation of RBC adhesion in whole blood samples. SCD may be an ideal disease with which to interrogate cellular adhesion as an indicator of disease activity and severity because point-of-care and real-time markers of disease activity are urgently needed.

In the 1980s, abnormal RBC adhesion in SCD was studied using flow chambers or ex vivo rat mesocecum.[52,59-61] However, cellular adhesion is not currently evaluated clinically because analyses of these cellular interactions are technically challenging and difficult to reproduce. Recently, microfluidic technologies have emerged as versatile platforms for diagnosing and monitoring diseases.[62-64] These devices allow simple and cost-efficient fabrication, short processing times, and minimal reagent use. Furthermore, microfluidic systems can be easily

adapted to mimic biophysical microenvironment of cells for a more comprehensive and accurate analysis of the subject's pathophysiological state.[65-68] Microfluidic platforms have been used in diagnosis and/or monitoring of several life-threatening diseases such as cancer,[67,69,70] human immunodeficiency virus,[71,72] and thrombosis.[73,74]

Here, we present a clinically relevant microfluidic device (SCD biochip) that allows serial quantitative measurements of RBC adhesion to endothelium-associated protein-immobilized microchannels (fibronectin [FN] or laminin [LN]) in a closed and preprocessing-free system. RBC deformability, when adhered, can also be evaluated using this technology. FN is a glycoprotein that circulates in plasma and is present in the endothelial cell membrane.[75,76] FN plays a role in SCD RBC adhesion, via RBC integrin $\alpha 4\beta 1$ (also known as very late antigen-4 or VLA-4 integrin) interaction[75,77,78] with the endothelial wall.[75,77,78] LN is subendothelial and binds to an important RBC surface protein from the immunoglobulin superfamily, BCAM/LU (basal cell adhesion molecule, Lutheran antigen),[59,79-82] which is phosphorylated during beta-adrenergic stimulation.[59,80-82] We have analyzed more than 100 subject blood samples using the SCD biochip, showing significant associations between RBC adhesion on FN and LN with hemoglobin (Hb) phenotype (HbSS, HbSC, and HbAA), fetal hemoglobin (HbF) levels; lactate dehydrogenase (LDH); platelet and reticulocyte counts. The SCD biochip allowed us to analyze RBC adhesion in a sizable, adult, well-phenotyped, SCD population.

METHODS

Study design. All attainment of samples and clinical information, such as laboratory tests, treatment courses, and medical history, was performed with informed consent of the subjects and under the institutional review board approval. It is standard of care for patients to get complete blood counts (CBCs) during routine (baseline) clinic visits. Blood samples from patients with HbSS, HbSC, HbSC/Sβ^+, and healthy controls (Hb AA) were de-identified and collected during the regular course of the Adult Sickle Cell Clinic at the University Hospitals Case Medical Center in Cleveland. Surplus blood samples, drawn in an ethylenediaminetetraacetic acid (EDTA)–containing Vacutainer ("purple top") tube, were obtained. A volume of 0.25-mL whole blood is used in the SCD biochip. All samples were run within 24 hours of acquisition. Collected data included Hb phenotype, CBC (including white blood cell [WBC, 10^9/L], red blood cell [10^{12}/L], absolute neutrophil count [10^6/L], platelet count [10^9/L], and reticulocyte count [10^9/L]), plasma LDH (U/L), and pain level (by FACES or numeric pain rating scale, between 0 [no pain] and 10 [worst possible pain]). Sample attainment relative to any treatments, such as hydroxyurea use or blood transfusions, was noted. Hb identification of Hb S, Hb F, Hb A, and Hb A2 was conducted via high-performance liquid chromatography (HPLC) at the Core Laboratory of University Hospitals Case Medical Center, using the Bio-Rad Variant II Instrument (Bio-Rad, Montreal, QC, Canada). Clinical laboratory values for subjects' blood samples are listed in Table I. Adults who were documented with SCD, including HbSS or compound heterozygous HbSC- or HbSβ-thalassemia diagnosis as evidenced by one or more clinical features, were assessed for eligibility (Fig S1). Written informed consent was obtained from the subjects who were able to comply with the requirements of the study. Presence of a condition or abnormality that, in the opinion of the investigator, would compromise the safety of the patient or researcher performing the experiment (such as infection) was regarded as an exclusion criterion. Control samples (HbAA) were obtained from Research Blood Components (Boston, MA) or from healthy volunteers. We recorded pain scores of patients in our study but did not rigorously assess temporal proximity to painful crises. Furthermore, any acutely ill patient was sent from our clinic to the day hospital for treatment, and those samples were not available for processing. We estimate that 5%–10% of patient visits were handled in this way. A subset of early samples was obtained anonymously without correlative clinical data beyond hemoglobin phenotype.

Table I. Clinical phenotype of the consented SCD patient population

	Mean ± SE	Range
Age	37.6 ± 2.5	19–72
WBC (10^9/L)	9.7 ± 0.6	4.1–22.6
Reticulocyte count (10^9/L)	324.1 ± 29.0	89–798
Hemoglobin (g/dL)	8.8 ± 0.3	5.5–12
Platelet count (10^9/L)	361.1 ± 22.7	155–703
Absolute neutrophil count (10^6/L)	4899.1 ± 459.7	720–14,240
Lactate dehydrogenase (U/L)	408.3 ± 32.7	157–934
Pain*	3.4 ± 0.5	0–10
Hemoglobin F (%)	9.8 ± 1.3	0.4–23.9
Hemoglobin S (%)	72.3 ± 3.2	17.6–91.1
Hemoglobin A (%)	10.9 ± 3.2	0–66.1

Abbreviations: SE, Standard error; *WBC*, white blood cell.
Data presented is based on 32 blood samples (n) from 27 consented SCD patients (male = 11, female = 16).
*"n" for pain score was 31.

Table II. Ability of SCD biochip in differentiating between hemoglobin phenotypes based on RBC adhesion to FN and LN microchannels

	FN			LN		
	SS-AA	SC-AA	SS-SC	SS-AA	SC-AA	SS-SC
Threshold	9	9	30	16	16	170
Sensitivity	0.93	0.80	0.75	0.93	0.89	0.87
Specificity	1.00	1.00	0.70	1.00	1.00	0.78
PLR	Inf	Inf	2.50	Inf	Inf	3.90
NLR	0.07	0.20	0.36	0.07	0.11	0.17
PPV	1.00	1.00	0.88	1.00	1.00	0.87
NPV	0.83	0.83	0.50	0.89	0.89	0.78
Accuracy	0.95	0.90	0.74	0.96	0.94	0.83
AUC	0.88	0.88	0.77	0.86	0.99	0.89

Abbreviations: AUC, Area under the receiver operating characteristic curve; *FN,* fibronectin; *LN,* laminin; *PLR,* positive likelihood ratio; *PPV,* positive predictive value; *NLR,* negative likelihood ratio; *NPV,* negative predictive value.
Threshold unit is number of adhered RBCs per unit area.

SCD biochip device fabrication. SCD biochip is designed and developed to mimic the physiological conditions of the microvasculature. The microfluidic devices are designed and fabricated to be single use to prevent cross-contamination between samples. Microfluidic channels are composed of a glass surface functionalized with FN or LN, a poly(methyl methacrylate) plastic top (encompassing inlets and outlets), and sandwiched 50-μm-thick double-sided adhesive tape that defined the height and shape of the microchannels (Fig S2). RBC adhesion to FN or LN was measured in SCD biochip, without preprocessing, at or above physiological flow shear stresses of postcapillary venules (1–5 dyne/cm^2),[53,83-85] ranging from 1 to 50 dyne/cm^2. Briefly, SCD biochip was fabricated by assembling poly(methyl methacrylate) top parts, cut by VersaLaser system (Universal Laser Systems Inc., Scottsdale, Ariz), and double-sided adhesive film (iTapestore, Scotch Plains, NJ) which have an inlet and outlet (0.61 mm in diameter and 26 mm apart).[68] They were placed onto Gold Seal glass slide (adhesion coating: APTES, 3-Aminopropyl Triethoxysilane, Electron Microscopy Sciences [Hatfield, Pa]). Surface chemistry inside microchannels was achieved by flushing the channels with N-g-Maleimidobutyryloxy succinimide ester (0.28% vol/vol) followed by incubation in FN (fibronectin from human plasma, 1:10; Sigma Aldrich, St Louis, Mo) or LN (laminin from Engelbreth-Holm-Swarm murine sarcoma basement membrane, LN 1, 1:10; Sigma Aldrich) for 1.5 hours at room temperature. Then, channels were incubated in bovine serum albumin solution (20 mg/mL) overnight at 4°C for blocking nonspecific binding events. After assembly of inlet and outlet tubing, undiluted whole blood samples from subjects were injected on to FN- or LN-immobilized microchannels at 18.5 μL/min to 25.8 μL/min to fill channels, then 1.85 μL/min (1 dyne/cm^2) to 2.58 μL/min (1.4 dyne/cm^2) until 15 μL of the sample was introduced. After the blood flow, 180 μL of flow cytometry staining buffer (FCSB, 1X, with albumin 0.5%–1%, without fluoresceinated antibodies) was run at 10 μL/min (1 dyne/cm^2) for 18 minutes in the channels, to remove non-adhered RBCs. All flow steps were conducted using New Era NE-300 syringe pump system (Farmingdale, NY). An inverted microscope (Olympus IX83) and microscopy camera (EXi Blue EXI-BLU-R-F-M-14-C) was used to obtain high-resolution images of whole channels. All experiments were conducted at room temperature.

Image processing and quantification. Whole phase-contrast images of microchannels with adhered RBCs are obtained using Olympus (20x/0.45 ph2 and 40x/0.75 ph3) long working distance objective lenses. Images were then processed using Adobe Photoshop software (San Jose, CA) for quantification of adhered RBCs per unit area (32 mm^2). Here, we categorized RBCs based on morphology as deformable RBCs with the characteristic biconcave shape and nondeformable RBCs lacking biconcave morphology, based on earlier work.[66]

Statistical analysis. The relationship between individual components of the CBC and serum tests and the number of adhered RBCs was analyzed using K-means clustering. The patients with HbSS were clustered into 2 groups, and the resultant groups were evaluated for differences in adhesion. Single and multiple components of the CBC and serum analyses were used to identify the 2 subgroups. Once the subgroups were identified by K-means clustering, the difference between the numbers of adhered RBCs between these groups was tested for statistical significance using the one-way analysis of variance (ANOVA) test. The testing level (alpha) was set as 0.05 (two-sided). The component or components that lead to the significant subgroups in terms of the differences between the numbers of adhered RBCs were reported in this article. The K-means clustering was performed using Matlab (The MathWorks, Inc, Natick, Mass). Receiver-operating curves were used to determine the SCD biochip's accuracy of differentiation between hemoglobin phenotypes. The curves were generated using Matlab (The MathWorks, Inc). In addition to the area under the curve, sensitivity, specificity, positive and negative likelihood ratios, and positive and negative predictive values were calculated as follows: Sensitivity was calculated as # true positives/(# true positives + #

false negatives), specificity as # true negatives/(# true negatives + # false positives). Positive likelihood ratio was defined as sensitivity/(1-specificity). Negative likelihood ratio was (1-sensitivity)/specificity. Positive predictive value was # true positives/(# true positives + # false positives), and negative predictive value was # true negatives/(# true negatives + # false negatives).

RESULTS

Probing abnormal RBC adhesion in a microfluidic channel. The SCD biochip affords quantitative analysis of RBCs with abnormal membrane and adhesive properties following attachment to endothelium-associated proteins (Fig 1, A). The number of adhered RBCs is quantified inside the FN- or LN-immobilized microfluidic channels. We observed abnormal adhesion of RBCs to the SCD biochip in blood samples from subjects with SCD (Fig 1, B). In contrast, adhesion of RBCs in blood samples from normal subjects was negligible (not shown). Different levels of RBC adhesion were observed in patients with various clinical phenotypes (Fig 1, C and D).

RBC adhesion varies among hemoglobin phenotypes. We analyzed the number of adhered RBCs per unit area (32 mm^2) in FN- and LN-functionalized parallel microchannels (Fig S2) in blood samples from subjects without SCD (HbAA), or with compound heterozygous (HbSC or HbSβ^+-thalassemia, HbSC/Sβ^+) or homozygous SCD (HbSS), using high-resolution images from microfluidic channels (Fig 2, A and B). RBC adhesion to FN- or LN-coated microchannels was highest in HbSS relative to HbSC/Sβ^+, and higher in HbSC/Sβ^+ relative to HbAA containing blood samples (Fig 2, C and D). Close-up views of adhered RBCs in functionalized microchannels are shown in Fig S3. For selected thresholds of adhered RBC numbers, we observed 0.93 true-positive rate and 0.00 false-positive rate for differentiating between HbSS and HbAA phenotypes (Fig 2, E and F). Area under the curve for differentiating between HbSS and HbAA was >0.85 both for FN and LN (Table II). The ROC were strongest in discriminating between AA and SS or SC, compared with discrimination between SS and SC. These results demonstrate the ability of the SCD biochip to discriminate among hemoglobin

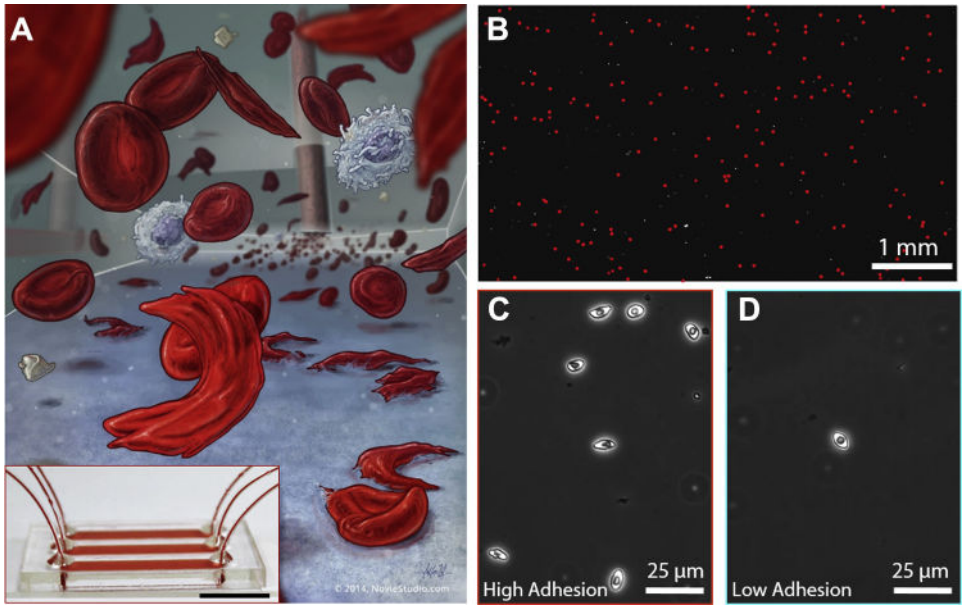

Fig 1. Sickle cell disease biochip (SCD biochip) probes red blood cell (RBC) adhesion in a closed system using minuscule amounts of whole blood samples. (**A**) Flow and RBC cell adhesion are illustrated inside the SCD biochip. Shown are varying levels of sickling and adherence to endothelium-associated protein-coated microchannel surfaces. (Inset) SCD biochip consists of multiple parallel microchannels. Scale bar represents a length of 10 mm. (**B**) Number of adhered RBCs are quantified inside microfluidic channels that are functionalized with FN or LN. We observed abnormal RBC adhesion in blood samples from SCD subjects. Adhered RBCs are marked with red dots. (**C** and **D**) High-resolution phase-contrast images of adhered RBCs with heterogeneous sickle morphologies inside the SCD biochip are shown. Different levels of RBC adhesion were observed in blood samples from patients with various clinical phenotypes, such as high or low hemoglobin F (HbF) levels. FN, Fibronectin; LN, laminin; RBC, red blood cell; SCD, sickle cell disease.

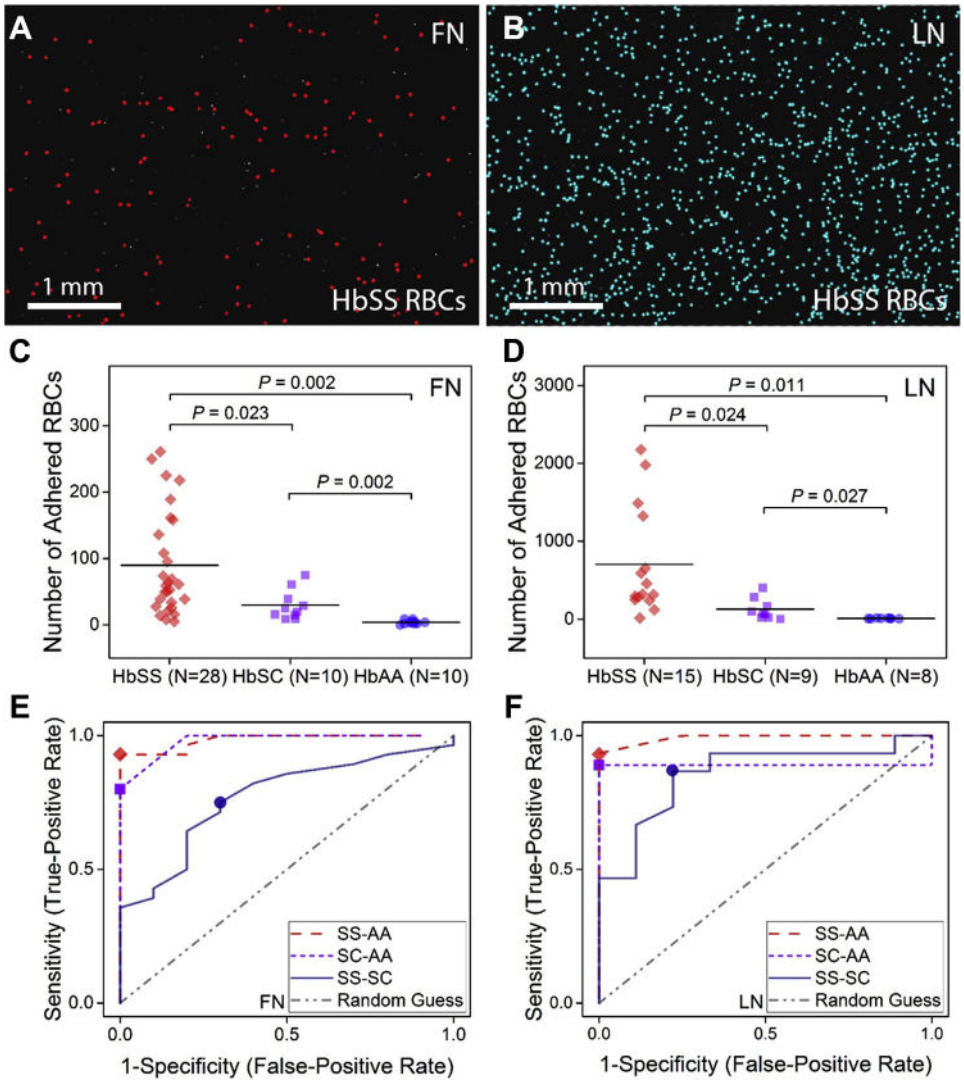

Fig 2. Adhesion of RBCs in FN- and LN-functionalized microchannels varies among SCD hemoglobin phenotypes and are greatest in HbSS. Shown are high resolution images of microchannels in (**A**) FN or (**B**) LN. The number of adhered RBCs was significantly higher in samples from subjects with HbSS > HbSC/Sβ^+ > HbAA in both (**C**) FN and (**D**) LN immobilized microchannels. The horizontal lines between individual groups represent a statistically significant difference based on a one-way ANOVA test ($P < 0.05$). Data point cross bars represent the mean. "N" represents the number of subjects. (**E** and **F**) Receiver operating-characteristic (ROC) curves display a true-positive rate (sensitivity) and a false-positive rate (1-specificity) for differentiation between SS-AA, SC-AA, and SS-SC hemoglobin phenotypes based on adhesion of RBCs to (**E**) FN and (**F**) LN. Defined thresholds for adhered RBC numbers on the ROC are as shown (◇ = 9 (SS-AA), □ = 9 (SC-AA), and ○ = 30 (SS-SC) for FN; ◇ = 16 (SS-AA), □ = 16 (SC-AA), and ○ = 170 (SS-SC) for LN). ANOVA, Analysis of variance; FN, fibronectin; LN, laminin; RBC, red blood cell; SCD, sickle cell disease.

phenotypes solely based on cellular adhesion. These data support the role that abnormal cellular adhesion plays in accounting for differences among SCD phenotypes. High levels of HbF are associated with improved clinical outcomes in SCD.[86] Therefore, we investigated RBC adhesion in HbSS blood samples with low (<%8) and high (>%8) HbF levels (Fig 3), based on estimates of what is physiologically relevant.[86] The mean number of adhered RBCs was significantly higher in blood samples from HbSS subjects with low HbF compared with those from subjects with high HbF levels, in both FN- (Fig 3, A) and LN-functionalized (Fig 3, B) microchannels. These results demonstrate that SCD biochip is a plausible in vitro adhesion assay for functional phenotypes of SCD.

Clinical correlates for RBC adhesion to FN and LN. We used K-means clustering analysis to identify subgroups

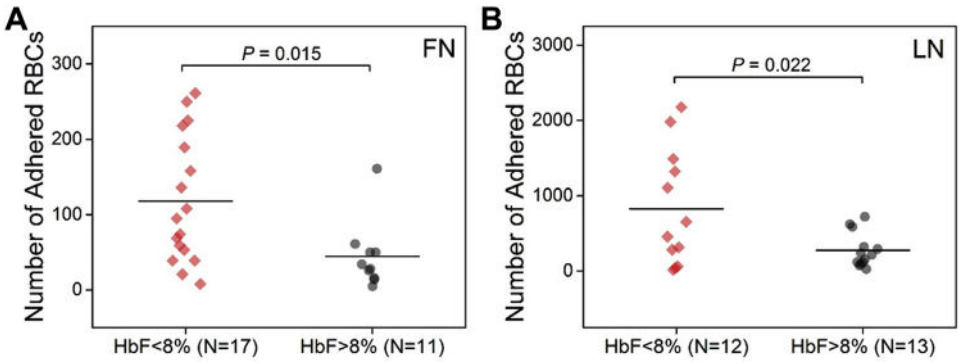

Fig 3. Adhesion of RBCs is greater in HbSS subjects with a low (<%8) HbF, compared with high (>%8) HbF. (**A** and **B**) RBC adhesion was quantified in blood samples of HbSS patients with high and low HbF levels, from temporally nearest clinical measurement (not uniformly contemporaneous). Number of adhered RBCs was significantly higher in blood samples from subjects with low HbF levels compared with blood samples from subjects with high HbF levels in both (**A**) FN and (**B**) LN immobilized microchannels. The horizontal lines between individual groups represent a statistically significant difference based on a one-way ANOVA test ($P < 0.05$). Data point cross bars represent the mean. "N" represents the number of subjects. ANOVA, Analysis of variance; FN, fibronectin; HbF, fetal hemoglobin; LN, laminin; RBC, red blood cell.

of HbSS patients based on individual components of standard blood tests. We analyzed HbSS RBC adhesion to FN microchannels in blood samples from patients with dichotomized laboratory values, including LDH levels and percent HbS. The mean adherence was directly associated with LDH levels (FN, Fig 4, A). K-means clustering analyses were then applied to determine univariate models with greater significance in correlation with RBC adhesion to FN. Levels of HbS varied due to recent transfusions (HbA ≥10%) or due to increased levels of HbF. High levels of HbS were associated with increased LDH levels (group 1 relative to group 2, Fig 4, B). We observed that patients with high HbF tended to have low serum LDH levels (14/16 patients with >%8 HbF have <500 U/L LDH; Fig S4). Adherence to FN was significantly greater in blood samples with higher LDH and higher HbS levels (group 1 compared with group 2, Fig 4, C). Most transfused subjects (7/9) were in the lower LDH subgroup (LDH <500 U/L, Fig S5). In addition, subjects with a lower platelet count (<320 10^9/L) consistently had fewer than 400 adherent RBCs per unit area of FN (Fig S6). These methods were also applied to determine correlations with RBC adhesion to LN (Fig 5). Adherence to LN was significantly greater in HbSS blood samples with higher LDH (Fig 5, A) or higher reticulocyte counts (Fig 5, B). High levels of LDH were associated with elevated reticulocyte counts (group 1 relative to group 2, Fig 5, C). In univariate models, we observed significantly greater adhesion to LN in HbSS blood samples with higher LDH and higher reticulocyte levels (group 1 compared with group 2, Fig 5, D), independent of HbS (Fig S5, C and D). Moreover, we analyzed correlation between RBC adhesion to FN and LN, and reticulocyte counts for SCD subjects (Fig S7). We found a statistically significant correlation between reticulocyte counts and RBC adhesion to LN (Pearson product-moment correlation coefficient, PCC = 0.53, $P = 0.007$) and to FN (PCC = 0.46, $P = 0.035$), and this effect was increased in the absence of transfused subjects for both LN (PCC = 0.72, $P < 0.0001$) and FN (PCC = 0.66, $P = 0.018$). Furthermore, we analyzed RBC counts of the patient blood samples used in our study and found an average number of $2.65 \pm 0.66 \times 10^9$ RBCs/mL (mean ± standard deviation, Fig S8, A), where 21 of 31 blood samples had RBC counts within $1.9–2.9 \times 10^9$ RBCs/mL. There was no statistically significant correlation between RBC counts of the blood samples and number of adhered RBCs to either FN or LN (Fig S8, B and C).

These results show clinical associations between RBC adhesion to FN or LN with LDH, platelet counts, or reticulocyte counts. Nonetheless, heterogeneity was present in all analyses, for example, low adhesion in some patients with a high LDH or elevated reticulocyte count (Figs 4 and 5); this was also seen in a subset of chronically transfused patients; the converse was less ambiguous, for example, low adhesion was present in most patients with a low LDH (Fig 4).

Identifying subpopulations of adherent RBCs. The morphology and number of adherent RBCs in HbSS blood samples were examined after controlled detachment of cells at step-wise increased flow shear stresses of 1, 4, and 50 dyne/cm^2 (Fig 6, A–C). Based on

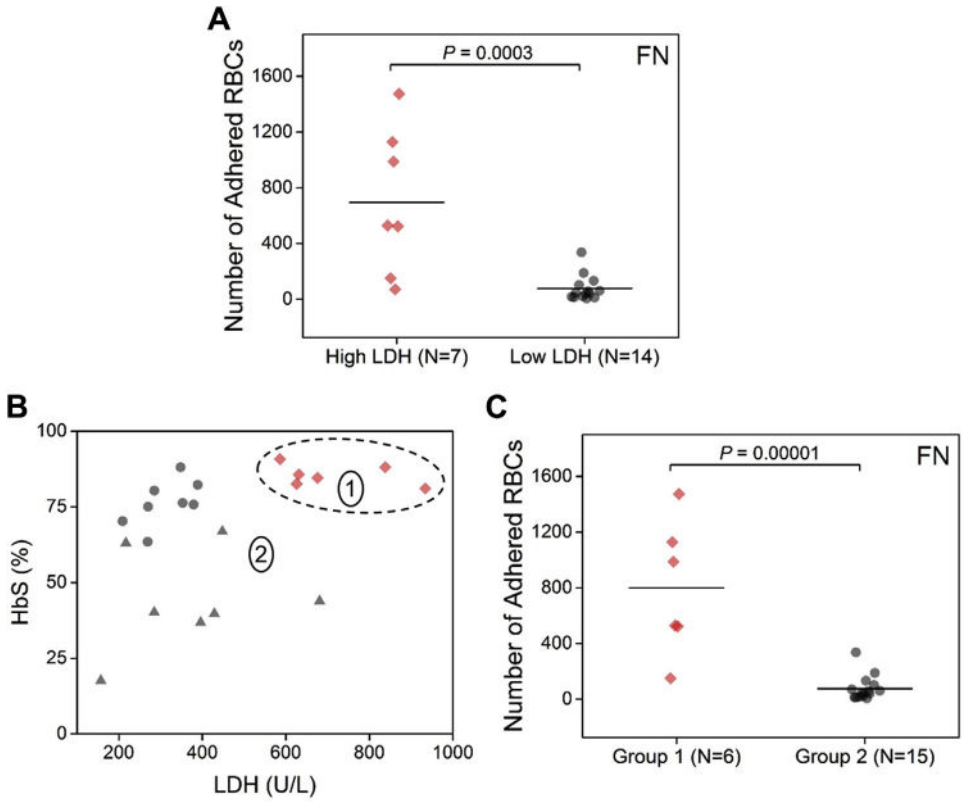

Fig 4. RBC adhesion to FN is associated with lactate dehydrogenase (LDH) and HbS percentage. (**A**) Number of adhered RBCs in FN microchannels was significantly higher in blood samples with high LDH (>500 U/L). Seven of 9 samples are from subjects who had recently been transfused (Fig S4) and who had low LDH and low adhesion. (**B**) In blood samples with higher LDH and higher HbS (group 1), determined by k-means clustering analysis, (**C**) adherence to FN was significantly greater compared with lower LDH and lower HbS (group 2). Samples from recently transfused subjects are shown with triangle markers. The horizontal lines between individual groups represent a statistically significant difference based on a one-way ANOVA test ($P < 0.05$). Data point cross bars represent the mean. "N" represents the number of subjects. ANOVA, Analysis of variance; FN, fibronectin; RBC, red blood cell.

morphologic characterization, adhered RBCs were categorized as deformable (Fig 6, D) or nondeformable (Fig 6, E), based on our earlier work.[66] The percent of deformable and nondeformable RBCs, relative to total adhered RBCs at 1 dyne/cm^2 shear stress, was calculated in each experiment, and the mean and standard error were determined (Fig 6, F). These analyses were repeated at higher shear stresses of 4 and 50 dyne/cm^2. The total number of adhered RBCs decreased with higher shear stresses, whereas the proportion of nondeformable RBCs increased in these same experiments (Fig 6, F). The percent of nondeformable RBCs, determined at 1 dyne/cm^2, correlated significantly with serum LDH levels in test subjects (Fig 6, G; PCC = 0.74; $P < 0.0001$). These results indicate a morphologic heterogeneity in adhered RBCs and suggest an association between LDH (an indicator of hemolysis) and adherent nondeformable RBCs. A detailed description of RBC adhesion at differing flow rates is shown in Fig S9, with close-up views of adhesion to FN and LN, respectively, in Figs S10 and S11.

Longitudinal analysis of RBC adhesion. We conducted longitudinal analyses on a limited number of individual subjects, performed ≥1 month apart using the same biomolecule, FN or LN (Fig S12). Stable SCD RBC adhesion to FN was seen in 2 patients being treated for SCD, including unique patient number (UPN) 21 (Fig S12, A), examined when HbA levels were stable on transfusions, and UPN 118, examined when HbF levels were stably elevated on hydroxyurea (Fig S12, A). Noted, but of unknown significance, since in 2 patients, is the overall lower adhesion seen in the subject on hydroxyurea, given the pancellular effects of hydroxyurea compared with transfusions. Adhesion to FN dropped after each transfusion in UPN 67, monitored over 6 months,

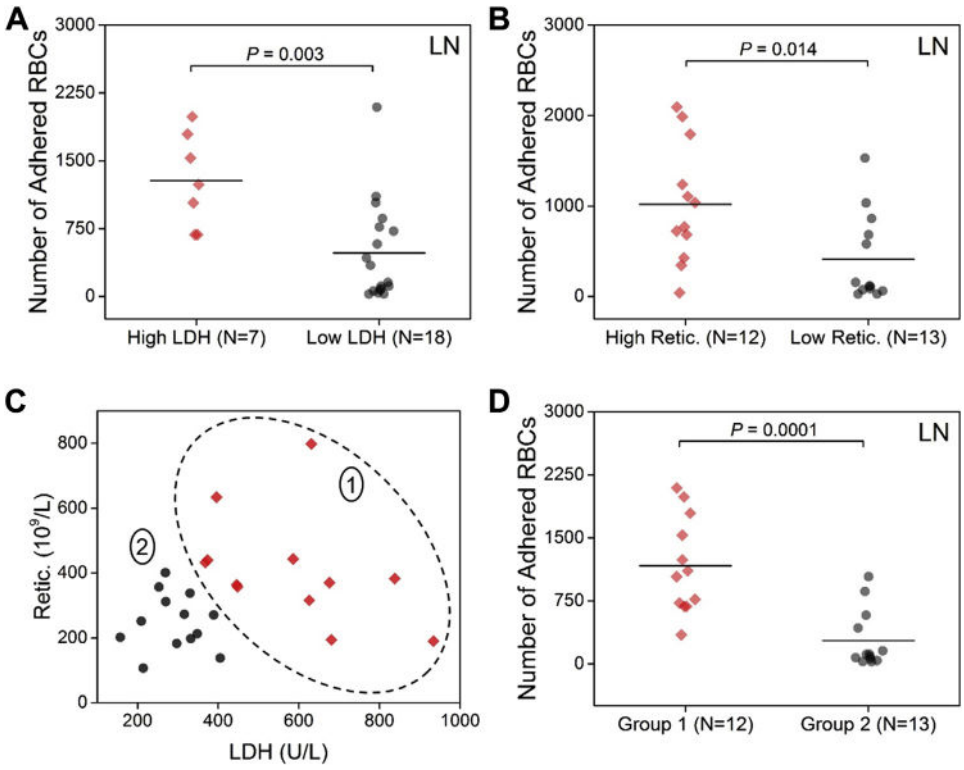

Fig 5. RBC adhesion to LN is associated with high LDH and high absolute reticulocyte counts. (**A** and **B**) RBCs in blood samples with (**A**) high LDH (>500 U/L) and (**B**) higher reticulocyte counts (>320 10^9/L) showed a significantly higher adherence to LN-immobilized microchannels compared with RBCs from samples with low LDH (<500 U/L) and low reticulocyte counts (<320 10^9/L), respectively. (**C**) Blood samples with higher LDH and higher reticulocyte counts (group 1), determined by k-means clustering analysis, (**D**) showed significantly greater adhesion to LN compared with blood samples with lower LDH and lower reticulocyte counts (group 2). The horizontal lines between individual groups represent a statistically significant difference based on a one-way ANOVA test ($P < 0.05$). Data point cross bars represent the mean. "N" represents the number of subjects. ANOVA, Analysis of variance; LDH, lactate dehydrogenase; LN, laminin; RBC, red blood cell.

after 2 episodes of transfusion (Fig S12, B). Adhesion to LN was stable in UPN 20, being managed with supportive care, and in UPN 35, stably on hydroxyurea (Fig S12, C). Adhesion to LN in a single patient dropped by >80% from baseline after initiation of hydroxyurea, as HbF rose from 1% to 20% (Fig S12, D).

DISCUSSION

The sickle hemoglobin mutation afflicts many millions of people worldwide and is associated with considerable morbidity and mortality.[86] Even though the molecular underpinnings of SCD were recognized more than 60 years ago,[87] there is no clear-cut molecular or biophysical markers through which to evaluate disease severity in the clinic. Biophysical phenomena, such as cell adhesion and deformability, reflect the multi-scale dimensions of SCD including molecular alterations, perturbed regulatory pathways, and cellular abnormalities. These are plausible biomarkers of disease activity and progression. RBC adhesion has been shown to be a critical biophysical factor involved in vaso-occlusion[52,53] and to correlate with disease severity.[10-12] However, studies of RBC adhesion in SCD have been primarily proof-of-concept rather than clinically applicable, due to requirements for complicated custom-designed systems, highly trained personnel, specially obtained blood samples, and extensive sample manipulation.[52,59-61] These significant technological barriers have hindered the widespread evaluation of RBC adhesion clinically or as a research tool. This has restricted our ability to integrate complex RBC adhesion phenomena into our understanding of SCD.

Here, we introduce a novel microfluidic biochip technology, SCD biochip, which provides an easy-to-use platform for probing RBC adhesion quantitatively in clinically available blood samples. The SCD biochip allows rapid, fully enclosed, and preprocessing-free analysis of blood samples, which affords simultaneous

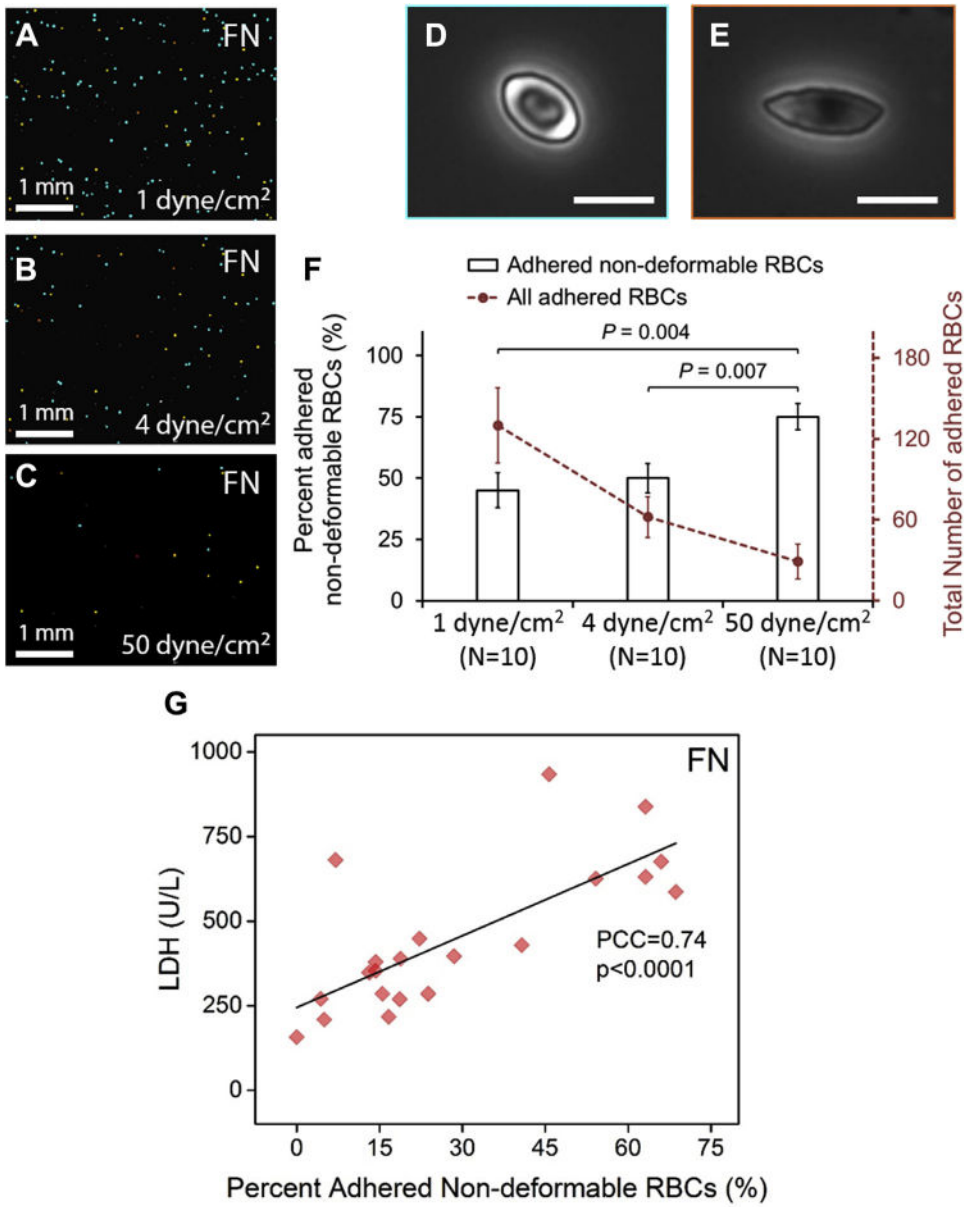

Fig 6. Heterogeneity in adhered RBCs in FN-functionalized microchannels is associated with serum LDH levels. (**A**–**C**) Number and morphology of adhered RBCs were analyzed in HbSS blood samples at step-wise increased flow shear stresses; (**A**) 1 dyne/cm^2, (**B**) 4 dyne/cm^2, and (**C**) 50 dyne/cm^2. (**D**) Deformable and (**E**) nondeformable RBCs were determined morphologically. Scale bars represent a length of 5 μm. (**F**) Nondeformable RBCs (% of total adhered RBCs) at 1, 4, and 50 dyne/cm^2 flow shear stress were calculated (columns). Total number of RBCs at each flow velocity is shown. The horizontal lines between individual groups represent a statistically significant difference based on a one-way ANOVA test ($P < 0.05$). Error bars represent the standard error of the mean. "N" represents the number of subjects. (**G**) Shown is adhered nondeformable RBCs (% of total) and serum LDH (U/L) at 1 dyne/cm^2 (Pearson correlation coefficient of 0.74, $P < 0.0001$, N = 21). ANOVA, Analysis of variance; FN, fibronectin; LDH, lactate dehydrogenase; RBC, red blood cell.

interrogation of both cellular behavior and plasma characteristics.[66] Cumulative membrane damage and aberrant activation of multiple adhesion receptors are acquired over the life of a HbS-containing RBC and cause abnormal adhesion. This integrates pathophysiological processes, that are both intracellular (eg, hemoglobin concentration, composition,[88-90] and polymerization[55,91]), and extracellular/plasma (eg, cytokines[92,93] or beta adrenergic stimulation[94,95]). The SCD biochip measures RBC adhesion quantitatively

in patients' whole blood samples without any preprocessing.

Blood flow in microcirculation is dependent on the intrinsic RBC biomechanical properties, namely deformability[96,97] and adhesiveness.[11,35,94] RBC deformability and adhesion are compromised in many disease states, resulting in blockages of blood flow in microcapillary networks. Abnormal RBC adhesion to endothelium has been implicated in other multisystem diseases, such as β-thalassemia, diabetes mellitus, hereditary spherocytosis, polycythemia vera, and malaria.[13,98,99] The precise contribution of different cell types to initiation and propagation of the vaso-occlusive crisis, which is pathophysiologically central to SCD, is unknown. We observed adhesion of different RBC subpopulations to FN and LN, reminiscent of RBC subpopulations defined in the literature for vaso-occlusion.[100] Furthermore, although deformable sickle RBCs adhere in higher numbers (especially to LN), nondeformable RBCs display greater adhesion strength, suggesting a critical contribution by both populations to vaso-occlusion.

RBC adhesion in SCD is governed by the complex interactions among RBC receptors, endothelial cell ligands, and plasma factors.[77,101-103] In this study, we functionalized microfluidic channels with FN or LN, which are known to be critical in RBC adhesion to endothelium.[56] FN is an adhesive glycoprotein that circulates in plasma and is present on the endothelial cell membrane.[78,102] FN is reported to interact with multiple RBC adhesion molecules, including CD44, CD147 (basigin/neurothelin), and $\alpha 4\beta 1$ integrin (VLA-4),[102] and with other plasma proteins, such as thrombospondin.[104,105] Furthermore, a primary role was suggested for FN in RBC adhesion during vascular injury or inflammation.[78,106] In our study, we used FN as an adhesion molecule based on multiple earlier in vitro[60,77,101] and ex vivo animal experiments,[106,107] suggesting a critical role of FN in mediating RBC adhesion.

LN is a subendothelial matrix protein that interacts with RBC BCAM/Lu.[56,108-110] This interaction has been attributed primarily to interactions with the $\alpha 5$ chain of LN subtypes 10/11,[102,111-113] although other investigators have described RBC- or BCAM/Lu-mediated interactions to human placental or non-10/11 LN subtypes,[59,108,111,114] including LN 1.[114] Human placental LN contains a mixture of LN isoforms, including LN 1, 2, 3, 4, and 10, and generally contaminated with FN, entactin, and collagen type IV.[111,115-117] Here, we observed adhesion of sickle RBCs to subtype LN 1 that is associated with clinical phenotype (increased LDH, reticulocytosis). Augmentation of sickle RBC binding in the presence of autologous plasma has been suggested for other RBC interactions,[103,118-120] and this effect may be at play in our system as well.

We used patient blood samples collected in Vacutainer tubes with EDTA. EDTA is the most widely used anticoagulant for blood collection.[121] Thus, we tested our SCD biochip technology with a standard blood collection method that is applicable to most clinical settings. The blood used in our studies, surplus from clinically obtained complete blood cell analyses, is easily attainable, due to the frequent use of this test in the clinical care of patients with SCD. To date, EDTA anti-coagulated blood has not appreciably affected analyses of RBC adhesion to FN or LN. In the future, we plan to use alternate anti-coagulants (eg, sodium citrate or corn trypsin inhibitor) with specially drawn blood samples for detailed pathophysiological analyses of RBC and WBC adhesion.

We showed significant associations between RBC adhesion and individual features of red cell phenotype, including hemoglobin content (HbSS, HbSC, HbAA, %HbF, %HbA), reticulocyte count, LDH; and RBC adhesion to FN and LN. These factors have known clinical relevance.[56,122-124] However, the relative contribution made by each RBC characteristic is not yet known. Furthermore, a range of hemoglobin phenotypes can be distinguished through the use of the SCD biochip. Greater adhesion of RBCs to endothelial cells or endothelium-associated proteins in HbSS blood samples compared with HbAA blood samples has been shown abundantly in the literature by a number of eminent researchers.[59,60,77,125-128] Moreover, RBC adhesion to FN and LN in patients undergoing hydroxyurea treatment was shown to decrease with increasing HbF levels.[110,126,129] Our results also showed greater adhesion of RBCs in HbSS blood samples compared with other hemoglobin phenotypes, and also in HbSS blood samples with lower HbF levels, which is in agreement with the previous studies.[59,60,77,110,125-127,129] However, to the best of our knowledge, there is no study reporting a side-by-side comparison of RBC adhesion from HbAA, HbSC, and HbSS patient blood samples using a standard adhesion assay and multiple adhesive interactions, as we have shown here. It is likely that useful insights about hemoglobin phenotype and disease severity may be gleaned from the SCD biochip, if applied widely.

Hemolysis has been identified as a central pathophysiological trigger in SCD, due to the deleterious impact of free heme on endothelial health and inflammation.[123,130-135] The relationship between RBC biophysical properties and hemolysis in SCD, including RBC adhesion and deformability, is not fully understood. Increased rigidity and cyclic sickling of

RBCs, resulting in cell membrane damage, has been suggested as the primary factor in intravascular hemolysis,[55,134,136,137] and it is possible that red cell adhesion may associate more strongly with hemolysis than with pain. Hemoglobin and arginase released from RBCs during hemolysis result in decreased nitric oxide bioactivity, affecting vascular tone and endothelial activation.[134,138] Markers of hemolysis in blood, such as LDH, have been associated with elevated soluble adhesion molecules in plasma, including Vascular Cell Adhesion Molecule 1 (VCAM-1), Intercellular Adhesion Molecule 1 (ICAM-1), P-selectin, E-selectin, and Von Willebrand factor.[123,138,139] Furthermore, significant correlations between percentage of dense and nondeformable RBCs and hemolysis markers, including bilirubin, aspartate transaminase, and LDH, have been shown.[13,140] Although an association between hemolysis and elevated plasma adhesion molecules has been shown before,[123,138,139] there is no report, to the best of our knowledge, that links hemolysis to adhesion and deformability of RBCs simultaneously. In this work, we identified a unique adherent nondeformable RBC population, significantly correlated with serum LDH levels, which reflects a functional outcome in terms of both deformability and adhesion of RBCs and is a pathophysiologically plausible source for active hemolysis in SCD. Of note, no single clinical characteristic (high LDH, increased reticulocytes, or low HbF) definitively identified high and low adhesion subgroups; we are working to develop better predictive models in the future, using multivariate analyses and larger patient numbers. Pain scores vary significantly from patient to patient at baseline.[141,142] Subjectivity in pain perception and variations in pain scores in SCD patients might contribute to the fact that we did not observe associations between pain scores and our measurements.

Understanding the pathophysiology of abnormal cell adhesion has allowed development of new pharmaceutical approaches, such as agents targeting platelet adhesion to Von Willebrand factor in atherosclerosis,[143,144] and blocking therapies inhibiting malaria-infected RBC adhesion to endothelial cells.[145] Quantitative assessment of cellular adhesion is a promising indicator of disease activity due to its integration of multiple scales of interrogation, from molecular to cellular interactions. This concept has been used in cancer[146] and atherosclerosis.[74,147] In parallel, microfluidic technologies developed recently have paved the way for widespread utilization of cellular adhesion as a clinical marker due to their ease of use, short analysis time, and enhanced capacity to mimic physiological conditions.[65-67] Hydroxyurea, the only approved pharmaceutical treatment for SCD, increases HbF content in the RBCs in some, but not all, treated subjects.[124] Hydroxyurea may decrease RBC adhesion through both HbF-inducing and non–HbF-inducing mechanisms.[92,113,126] One quarter of all samples with high HbF (>8%), used in our studies, were obtained from patients with hereditary persistence of HbF. Furthermore, our description of an association between lesser RBC adhesion and higher HbF% is congruent with the observation that increased HbF content interferes with polymerization of sickle hemoglobin molecules and mitigates the effects of the disease. The contribution to this effect that is attributable to non–HbF-related effects of hydroxyurea cannot be discerned in our current analyses.

Recently, extraordinary efforts have been made to transform current knowledge about abnormal cellular adhesion in SCD into clinical benefit for patients using novel targeted agents. VLA-4 blocking antibodies have been proposed in SCD.[148] Beta-adrenergic receptor blockade, which targets epinephrine-mediated red cell adhesion,[95,149-152] has been used in patients, using an U.S. Food and Drug Administration (FDA) approved medication (propranolol).[153] Red cell adhesion to an activated endothelium has specifically been targeted with small molecules ($\alpha_V\beta_3$),[154] low-molecular-weight heparin (P-Selectin),[155,156] and an oral agent in phase I/II studies in humans (P-selectin).[125,157,158] Abnormal interactions between leukocytes and activated endothelium and endothelial selectins have been targeted in vitro and in vivo with antibodies and small molecules[159-162] and are now the focus of phase II and III clinical studies in SCD. Although both P-selectin and E-selectin are important for adhesion of leukocytes to the endothelium, endothelial E-selectin appears crucial for generating secondary activating signals in the leukocyte.[163] The novel synthetic pan-selectin inhibitor, GMI-1070, with maximal activity against E-selectin has made it possible to test this paradigm in vivo in crisis.[162,164] Furthermore, a clinical trial using intravenous immunoglobulin infusions to block FcγRIII receptor mediation of secondary activity on neutrophils in children with SCD in crisis is in process (ClinicalTrials.gov identifier: NCT01757418).[165] A functional in-vitro adhesion test, such as the SCD biochip, could be a useful tool for measuring patients' response to treatment. Moreover, the SCD biochip could be adopted as an in-vitro model in which to test therapeutics that target cellular adhesion.

Key clinical and experimental studies, using flow chambers or ex vivo rat mesocecum,[52,59-61] have shown that sickle RBC adhesion and deformability, WBC adhesion and activation,[166] and aberrant endothelial activation all plausibly contribute to the

pathogenesis of vaso-occlusive crisis[52,53,125,155] and may correlate with disease severity.[10-12] Besides FN and LN, sickle RBC adhesion to other endothelium receptors, such as p-selectin, $\alpha_v\beta_3$ integrin, and VCAM-1, has been presented in the literature.[53,125,151] Monocytes[167-170] and neutrophils[171-173] are often increased in number, abnormally activated, and associated with adverse outcomes in SCD.[130,170,174-176] Quantitative abnormalities in lymphocytes and natural killer cells have been described[154,177] and are the focus of recent therapeutic interventions.[160,178] Perspectives on SCD pathophysiology must, in addition to RBC abnormalities, also integrate endothelial, WBC, and platelet activation and adhesion, inflammation, and thrombophilia.[167,172,179-189] Our work is not meant to be an exhaustive survey of all potential abnormal cellular adhesion events in SCD. The new SCD biochip platform, introduced here, has the potential to informatively interrogate leukocyte adhesion, leukocyte activation, and RBC adhesion to other endothelial surface proteins, which we will incorporate in future studies.

Despite recent advances in identifying and targeting cellular adhesion in SCD, knowledge about biophysical properties of abnormal cellular adhesion has not been integrated into routine clinical care or trial design, due to a requirement for complicated custom-designed systems, highly trained personnel, specially obtained blood samples, and extensive sample manipulation. SCD biochip will provide a more precise characterization of abnormal adhesive events in a given individual and may allow a more accurate assessment of response to therapy, especially emerging adhesive therapies, overall. Our goal is to make the SCD biochip as feasible, and clinically meaningful in SCD as glucose testing is in diabetes.

The SCD biochip is an in vitro assay for quantitative assessment of RBC adhesion, which has potential for on-site monitoring of disease activity and vaso-occlusion. The SCD biochip is feasibly applicable to a range of "real-world" clinical scenarios, having been tested using surplus blood obtained from a busy urban SCD clinic, at baseline and during clinical flux (including promising initial studies after treatment and in association with long-term complications). Our expectation is that longitudinal interrogations of cellular adhesion with the SCD biochip will be informative about physiological changes in patients over time during the clinical course of SCD.

ACKNOWLEDGMENTS

This work was supported by grant # 2013126 from the Doris Duke Charitable Foundation. The authors thank Dr MaryAnn O'Riordan for insightful discussions regarding data analysis and presentation. The authors acknowledge Cleveland Institute of Art Professor, Thomas Nowacki, for crafting the scientific illustration in Fig 1. U. A. Gurkan thanks the Case Western Reserve University, University Center for Innovation in Teaching and Education (UCITE) for the Glennan Fellowship, which supports the scientific art program and art student internship in Case Biomanufacturing and Microfabrication Laboratory. The authors acknowledge with gratitude the contributions of patients and clinicians at Seidman Cancer Center (University Hospitals, Cleveland). Editorial support was not used in preparation of this article.

Conflicts of Interest: The authors declare no financial interest. A patent application pertaining to the results presented in this article has been filed: Patent Cooperation Treaty Application (PCT/US2015/042907): "Biochips to Diagnose Hemoglobin Disorders and Monitor Blood Cells." All authors are aware of the journal's policy on disclosure of potential conflicts of interest.

Author contributions are as follows: Y. Alapan, J. A. Little, and U. A. Gurkan developed the idea. Y. Alapan, C. Kim, J. A. Little, and U. A. Gurkan designed the experiments. Y. Alapan, A. Adhikari, and C. Kim performed the experiments. Y. Alapan, C. Kim, A. Adhikari, K. E. Gray, E. Gurkan-Cavusoglu, and U. A. Gurkan analyzed the results. Y. Alapan, C. Kim, K. E. Gray, and U. A. Gurkan prepared the figures and the supplementary materials. Y. Alapan, C. Kim, E. Gurkan-Cavusoglu, J. A. Little, and U. A. Gurkan wrote the article.

REFERENCES

1. Sprague RS, Stephenson AH, Ellsworth ML. Red not dead: signaling in and from erythrocytes. Trends Endocrinol Metab 2007;18:350–5.
2. Mohandas N, Gallagher PG. Red cell membrane: past, present, and future. Blood 2008;112:3939–48.
3. Meredith JE, Fazeli B, Schwartz MA. The extracellular-matrix as a cell-survival factor. Mol Biol Cell 1993;4:953–61.
4. Skalak R, Branemar PI. Deformation of red blood cells in capillaries. Science 1969;164:717–9.
5. Canham PB, Burton AC. Distribution of size and shape in populations of normal human red cells. Circ Res 1968;22: 405–22.
6. Gauthier E, El Nemer W, Wautier MP, et al. Role of the interaction between Lu/BCAM and the spectrin-based membrane skeleton in the increased adhesion of hereditary spherocytosis red cells to laminin. Br J Haematol 2010;148: 456–65.
7. Moyer JD, Nowak RB, Kim NE, et al. Tropomodulin 1-null mice have a mild spherocytic elliptocytosis with appearance of tropomodulin 3 in red blood cells and disruption of the membrane skeleton. Blood 2010;116:2590–9.
8. Liu SC, Derick LH, Palek J. Visualization of the hexagonal lattice in the erythrocyte membrane skeleton. J Cell Biol 1987;104: 527–36.

9. Byers TJ, Branton D. Visualization of the protein associations in the erythrocyte membrane skeleton. Proc Natl Acad Sci U S A 1985;82:6153–7.
10. Hebbel RP. Adhesive interactions of sickle erythrocytes with endothelium. J Clin Invest 1997;100:S83–6.
11. Hebbel RP, Boogaerts MA, Eaton JW, Steinberg MH. Erythrocyte adherence to endothelium in sickle-cell anemia. A possible determinant of disease severity. N Engl J Med 1980;302:992–5.
12. Ballas SK, Smith ED. Red blood cell changes during the evolution of the sickle cell painful crisis. Blood 1992;79:2154–63.
13. Connes P, Lamarre Y, Waltz X, et al. Haemolysis and abnormal haemorheology in sickle cell anaemia. Br J Haematol 2014;165:564–72.
14. Lamarre Y, Romana M, Lemonne N, et al. Alpha thalassemia protects sickle cell anemia patients from macro-albuminuria through its effects on red blood cell rheological properties. Clin Hemorheol Microcirc 2014;57:63–72.
15. Baskurt OK, Gelmont D, Meiselman HJ. Red blood cell deformability in sepsis. Am J Respir Crit Care Med 1998;157:421–7.
16. Poschl JM, Leray C, Ruef P, Cazenave JP, Linderkamp O. Endotoxin binding to erythrocyte membrane and erythrocyte deformability in human sepsis and in vitro. Crit Care Med 2003;31:924–8.
17. Chandramohanadas R, Park Y, Lui L, et al. Biophysics of malarial parasite exit from infected erythrocytes. PLoS One 2011;6:e20869.
18. Hosseini SM, Feng JJ. How malaria parasites reduce the deformability of infected red blood cells. Biophys J 2012;103:1–10.
19. Nuchsongsin F, Chotivanich K, Charunwatthana P, et al. Effects of malaria heme products on red blood cell deformability. Am J Trop Med Hyg 2007;77:617–22.
20. Maier AG, Cooke BM, Cowman AF, Tilley L. Malaria parasite proteins that remodel the host erythrocyte. Nat Rev Microbiol 2009;7:341–54.
21. Spengler MI, Svetaz MJ, Leroux MB, Bertoluzzo SM, Parente FM, Bosch P. Lipid peroxidation affects red blood cells membrane properties in patients with systemic lupus erythematosus. Clin Hemorheol Microcirc 2014;58:489–95.
22. Ghiran IC, Zeidel ML, Shevkoplyas SS, Burns JM, Tsokos GC, Kyttaris VC. Systemic lupus erythematosus serum deposits C4d on red blood cells, decreases red blood cell membrane deformability, and promotes nitric oxide production. Arthritis Rheum 2011;63:503–12.
23. Kim CB, Shin S, Song SH. Hemorheological changes caused by lead exposure. Clin Hemorheol Microcirc 2013;55:341–8.
24. Lim KM, Kim S, Noh JY, et al. Low-level mercury can enhance procoagulant activity of erythrocytes: a new contributing factor for mercury-related thrombotic disease. Environ Health Perspect 2010;118:928–35.
25. Relevy H, Koshkaryev A, Manny N, Yedgar S, Barshtein G. Blood banking-induced alteration of red blood cell flow properties. Transfusion 2008;48:136–46.
26. Obrador R, Musulin S, Hansen B. Red blood cell storage lesion. Journal of Veterinary Emergency and Critical Care (San Antonio, Tex : 2001) 2015;25:187–99.
27. Adak S, Chowdhury S, Bhattacharyya M. Dynamic and electrokinetic behavior of erythrocyte membrane in diabetes mellitus and diabetic cardiovascular disease. Biochimica et biophysica acta 2008;1780:108–15.
28. Tsukada K, Sekizuka E, Oshio C, Minamitani H. Direct measurement of erythrocyte deformability in diabetes mellitus with a transparent microchannel capillary model and high-speed video camera system. Microvasc Res 2001;61:231–9.
29. Mercke CE. Anaemia in patients with solid tumours and the role of erythrocyte deformability. Br J Cancer 1981;44:425–32.
30. von Tempelhoff GF, Nieman F, Heilmann L, Hommel G. Association between blood rheology, thrombosis and cancer survival in patients with gynecologic malignancy. Clin Hemorheol Microcirc 2000;22:107–30.
31. Vos FE, Schollum JB, Coulter CV, Doyle TC, Duffull SB, Walker RJ. Red blood cell survival in long-term dialysis patients. Am J Kidney Dis 2011;58:591–8.
32. Nguyen DB, Wagner-Britz L, Maia S, et al. Regulation of phosphatidylserine exposure in red blood cells. Cell Physiol Biochem 2011;28:847–56.
33. Lang E, Qadri SM, Lang F. Killing me softly—suicidal erythrocyte death. Int J Biochem Cell Biol 2012;44:1236–43.
34. Forman S, Bischel M, Hochstein P. Erythrocyte deformability in uremic hemodialyzed patients. Ann Intern Med 1973;79:841–3.
35. Bonomini M, Sirolli V, Gizzi F, Di Stante S, Grilli A, Felaco M. Enhanced adherence of human uremic erythrocytes to vascular endothelium: role of phosphatidylserine exposure. Kidney Int 2002;62:1358–63.
36. Porro B, Eligini S, Squellerio I, Tremoli E, Cavalca V. The red blood cell: a new key player in cardiovascular homoeostasis? Focus on the nitric oxide pathway. Biochem Soc Trans 2014;42:996–1000.
37. Gaillard CA, Schiffelers RM. Red blood cell: barometer of cardiovascular health? Cardiovasc Res 2013;98:3–4.
38. Solá E, Vayá A, Martínez M, et al. Erythrocyte membrane phosphatidylserine exposure in obesity. Obesity 2009;17:318–22.
39. Samocha-Bonet D, Ben-Ami R, Shapira I, et al. Flow-resistant red blood cell aggregation in morbid obesity. Int J Obes 2004;28:1528–34.
40. Mokken FC, Kedaria M, Henny CP, Hardeman MR, Gelb AW. The clinical importance of erythrocyte deformability, a hemorheological parameter. Ann Hematol 1992;64:113–22.
41. Simpson LO, Shand BI, Olds RJ, Larking PW, Arnott MJ. Red cell and hemorheological changes in multiple sclerosis. Pathology 1987;19:51–5.
42. Sabolovic D, Roudier M, Boynard M, et al. Membrane modifications of red blood cells in Alzheimer's disease. J Gerontol 1997;52:B217–20.
43. Caspary EA, Sewell F, Field EJ. Red blood cell fragility in multiple sclerosis. British Medical Journal 1967;2:610–1.
44. Wild S, Roglic G, Green A, Sicree R, King H. Global prevalence of diabetes: estimates for the year 2000 and projections for 2030. Diabetes Care 2004;27:1047–53.
45. Laslett LJ, Alagona P, Clark BA, et al. The worldwide environment of cardiovascular disease: prevalence, diagnosis, therapy, and policy issues: a report from the American College of Cardiology. J Am Coll Cardiol 2012;60:S1–49.
46. Jha V, Garcia-Garcia G, Iseki K, et al. Chronic kidney disease: global dimension and perspectives. Lancet 2013;382:260–72.
47. Tchounwou PB, Yedjou CG, Patlolla AK, Sutton DJ. Heavy metal toxicity and the environment. EXS 2012;101:133–64.
48. Kassebaum NJ, Jasrasaria R, Naghavi M, et al. A systematic analysis of global anemia burden from 1990 to 2010. Blood 2014;123:615–24.
49. Jawad I, Luksic I, Rafnsson SB. Assessing available information on the burden of sepsis: global estimates of incidence, prevalence and mortality. Journal of Global Health 2012;2:010404.
50. Danchenko N, Satia JA, Anthony MS. Epidemiology of systemic lupus erythematosus: a comparison of worldwide disease burden. Lupus 2006;15:308–18.
51. Aarli JA, Dua T, Janca A, Muscetta A. Neurological disorders: public health challenges. World Health Organization 2006.

52. Kaul DK, Fabry ME, Nagel RL. Microvascular sites and characteristics of sickle cell adhesion to vascular endothelium in shear flow conditions: pathophysiological implications. Proc Natl Acad Sci U S A 1989;86:3356–60.
53. Kaul DK, Finnegan E, Barabino GA. Sickle red cell-endothelium interactions. Microcirculation 2009;16:97–111.
54. Potoka KP, Gladwin MT. Vasculopathy and pulmonary hypertension in sickle cell disease. Am J Physiol-Lung Cell Mol Physiol 2015;308:L314–24.
55. Barabino GA, Platt MO, Kaul DK. Sickle cell biomechanics. Annu Rev Biomed Eng 2010;12:345–67.
56. Stuart MJ, Nagel RL. Sickle-cell disease. Lancet 2004;364:1343–60.
57. Wood DK, Soriano A, Mahadevan L, Higgins JM, Bhatia SN. A biophysical indicator of vaso-occlusive risk in sickle cell disease. Sci Transl Med 2012;4:123ra26.
58. Ballas SK. The cost of health care for patients with sickle cell disease. Am J Hematol 2009;84:320–2.
59. Hillery CA, Du MC, Montgomery RR, Scott JP. Increased adhesion of erythrocytes to components of the extracellular matrix: isolation and characterization of a red blood cell lipid that binds thrombospondin and laminin. Blood 1996;87:4879–86.
60. Montes RA, Eckman JR, Hsu LL, Wick TM. Sickle erythrocyte adherence to endothelium at low shear: role of shear stress in propagation of vaso-occlusion. Am J Hematol 2002;70:216–27.
61. Barabino GA, McIntire LV, Eskin SG, Sears DA, Udden M. Endothelial cell interactions with sickle cell, sickle trait, mechanically injured, and normal erythrocytes under controlled flow. Blood 1987;70:152–7.
62. Whitesides GM. The origins and the future of microfluidics. Nature 2006;442:368–73.
63. Alapan Y, Icoz K, Gurkan UA. Micro- and nanodevices integrated with biomolecular probes. Biotechnology Advances 2015;33:1727–43.
64. Alapan Y, Hasan MN, Shen R, Gurkan UA. Three-dimensional printing based hybrid manufacturing of microfluidic devices. Journal of Nanotechnology in Engineering and Medicine. 6 (2):021007−021007-9.
65. Rizvi I, Gurkan UA, Tasoglu S, et al. Flow induces epithelial-mesenchymal transition, cellular heterogeneity and biomarker modulation in 3D ovarian cancer nodules. Proc Natl Acad Sci U S A 2013;110:E1974–83.
66. Alapan Y, Little JA, Gurkan UA. Heterogeneous red blood cell adhesion and deformability in sickle cell disease. Sci Rep 2014;4:7173.
67. Nagrath S, Sequist LV, Maheswaran S, et al. Isolation of rare circulating tumour cells in cancer patients by microchip technology. Nature 2007;450:1235–9.
68. Alapan Y, Matsuyama Y, Little JA, Gurkan UA. Dynamic deformability of sickle red blood cells in microphysiological flow. Technology 2016;0:1–9.
69. Karabacak NM, Spuhler PS, Fachin F, et al. Microfluidic, marker-free isolation of circulating tumor cells from blood samples. Nat Protoc 2014;9:694–710.
70. Chang CL, Huang W, Jalal SI, et al. Circulating tumor cell detection using a parallel flow micro-aperture chip system. Lab Chip 2015;15:1677–88.
71. Cheng X, Irimia D, Dixon M, et al. A microfluidic device for practical label-free CD4(+) T cell counting of HIV-infected subjects. Lab Chip 2007;7:170–8.
72. Moon S, Gurkan UA, Blander J, et al. Enumeration of CD4+ T-cells using a portable microchip count platform in Tanzanian HIV-infected patients. PLoS One 2011;6:e21409.
73. Branchford BR, Ng CJ, Neeves KB, Di Paola J. Microfluidic technology as an emerging clinical tool to evaluate thrombosis and hemostasis. Thromb Res 2015;136:13–9.
74. Foster GA, Gower RM, Stanhope KL, Havel PJ, Simon SI, Armstrong EJ. On-chip phenotypic analysis of inflammatory monocytes in atherogenesis and myocardial infarction. Proc Natl Acad Sci U S A 2013;110:13944–9.
75. Wick TM, Eckman JR. Molecular basis of sickle cell-endothelial cell interactions. Curr Opin Hematol 1996;3:118–24.
76. Mosher DF. Physiology of fibronectin. Annu Rev Med 1984;35:561–75.
77. Kasschau MR, Barabino GA, Bridges KR, Golan DE. Adhesion of sickle neutrophils and erythrocytes to fibronectin. Blood 1996;87:771–80.
78. Kumar A, Eckmam JR, Swerlick RA, Wick TM. Phorbol ester stimulation increases sickle erythrocyte adherence to endothelium: a novel pathway involving alpha 4 beta 1 integrin receptors on sickle reticulocytes and fibronectin. Blood 1996;88:4348–58.
79. Maciaszek JL, Andemariam B, Huber G, Lykotrafitis G. Epinephrine modulates BCAM/Lu and ICAM-4 expression on the sickle cell trait red blood cell membrane. Biophys J 2012;102:1137–43.
80. Benovic JL. Novel beta2-adrenergic receptor signaling pathways. J Allergy Clin Immunol 2002;110:S229–35.
81. Eyler CE, Jackson T, Elliott LE, et al. beta(2)-Adrenergic receptor and adenylate cyclase gene polymorphisms affect sickle red cell adhesion. Br J Haematol 2008;141:105–8.
82. Gauthier E, Rahuel C, Wautier MP, et al. Protein kinase A-dependent phosphorylation of Lutheran/basal cell adhesion molecule glycoprotein regulates cell adhesion to laminin alpha5. J Biol Chem 2005;280:30055–62.
83. Sheikh S, Rainger GE, Gale Z, Rahman M, Nash GB. Exposure to fluid shear stress modulates the ability of endothelial cells to recruit neutrophils in response to tumor necrosis factor-alpha: a basis for local variations in vascular sensitivity to inflammation. Blood 2003;102:2828–34.
84. Shaik SS, Soltau TD, Chaturvedi G, et al. Low intensity shear stress increases endothelial ELR+ CXC chemokine production via a focal adhesion kinase-p38{beta} MAPK-NF-{kappa}B pathway. J Biol Chem 2009;284:5945–55.
85. Kang H, Kwak HI, Kaunas R, Bayless KJ. Fluid shear stress and sphingosine 1-phosphate activate calpain to promote membrane type 1 matrix metalloproteinase (MT1-MMP) membrane translocation and endothelial invasion into three-dimensional collagen matrices. J Biol Chem 2011;286:42017–26.
86. Platt OS, Brambilla DJ, Rosse WF, et al. Mortality in sickle cell disease. Life expectancy and risk factors for early death. N Engl J Med 1994;330:1639–44.
87. Pauling L, Itano HA, Singer SJ, Wells IC. Sickle cell anemia a molecular disease. Science 1949;110:543–8.
88. Fathallah H, Atweh GF. Induction of fetal hemoglobin in the treatment of sickle cell disease. Hematology Am Soc Hematol Educ Program 2006;58–62.
89. Sauntharajah Y, Hillery CA, Lavelle D, et al. Effects of 5-aza-2'-deoxycytidine on fetal hemoglobin levels, red cell adhesion, and hematopoietic differentiation in patients with sickle cell disease. Blood 2003;102:3865–70.
90. Setty BN, Kulkarni S, Dampier CD, Stuart MJ. Fetal hemoglobin in sickle cell anemia: relationship to erythrocyte adhesion markers and adhesion. Blood 2001;97:2568–73.
91. Steinberg MH. Management of sickle cell disease. N Engl J Med 1999;340:1021–30.

92. Johnson C, Telen MJ. Adhesion molecules and hydroxyurea in the pathophysiology of sickle cell disease. Haematologica 2008;93:481–5.
93. Natarajan M, Udden MM, McIntire LV. Adhesion of sickle red blood cells and damage to interleukin-1 beta stimulated endothelial cells under flow in vitro. Blood 1996;87:4845–52.
94. Zennadi R, Whalen EJ, Soderblom EJ, et al. Erythrocyte plasma membrane-bound ERK1/2 activation promotes ICAM-4-mediated sickle red cell adhesion to endothelium. Blood 2012;119:1217–27.
95. Hines PC, Zen Q, Burney SN, et al. Novel epinephrine and cyclic AMP-mediated activation of BCAM/Lu-dependent sickle (SS) RBC adhesion. Blood 2003;101:3281–7.
96. Mohandas N, Clark MR, Jacobs MS, Shohet SB. Analysis of factors regulating erythrocyte deformability. J Clin Invest 1980;66:563–73.
97. Chien S. Red cell deformability and its relevance to blood flow. Annu Rev Physiol 1987;49:177–92.
98. Colin Y, Le Van Kim C, El Nemer W. Red cell adhesion in human diseases. Curr Opin Hematol 2014;21:186–92.
99. Cooke BM, Morrisjones S, Greenwood BM, Nash GB. Adhesion of parasitized red blood cells to cultured endothelial cells: a flow-based study of isolates from Gambian children with falciparum malaria. Parasitology 1993;107:359–68.
100. Manwani D, Frenette PS. Vaso-occlusion in sickle cell disease: pathophysiology and novel targeted therapies. Blood 2013;122:3892–8.
101. Manodori AB. Sickle erythrocytes adhere to fibronectin-thrombospondin-integrin complexes exposed by thrombin-induced endothelial cell contraction. Microvasc Res 2001;61:263–74.
102. Cartron JP, Elion J. Erythroid adhesion molecules in sickle cell disease: effect of hydroxyurea. Transfus Clin Biol 2008;15:39–50.
103. Hebbel RP. Adhesion of sickle red cells to endothelium: myths and future directions. Transfus Clin Biol 2008;15:14–8.
104. Lahav J, Lawler J, Gimbrone MA. Thrombospondin interactions with fibronectin and fibrinogen. Mutual inhibition in binding. European Journal of Biochemistry/FEBS 1984;145:151–6.
105. Dardik R, Lahav J. Multiple domains are involved in the interaction of endothelial cell thrombospondin with fibronectin. European Journal of Biochemistry/FEBS 1989;185:581–8.
106. Lutty GA, Taomoto M, Cao J, et al. Inhibition of TNF-alpha-induced sickle RBC retention in retina by a VLA-4 antagonist. Invest Ophthalmol Vis Sci 2001;42:1349–55.
107. Lutty GA, Otsuji T, Taomoto M, et al. Mechanisms for sickle red blood cell retention in choroid. Curr Eye Res 2002;25:163–71.
108. Udani M, Zen Q, Cottman M, et al. Basal cell adhesion molecule/lutheran protein. The receptor critical for sickle cell adhesion to laminin. J Clin Invest 1998;101:2550–8.
109. Zen Q, Cottman M, Truskey G, Fraser R, Telen MJ. Critical factors in basal cell adhesion molecule/lutheran-mediated adhesion to laminin. J Biol Chem 1999;274:728–34.
110. Hillery CA, Du MC, Wang WC, Scott JP. Hydroxyurea therapy decreases the in vitro adhesion of sickle erythrocytes to thrombospondin and laminin. Br J Haematol 2000;109:322–7.
111. Lee SP, Cunningham ML, Hines PC, Joneckis CC, Orringer EP, Parise LV. Sickle cell adhesion to laminin: potential role for the alpha5 chain. Blood 1998;92:2951–8.
112. Parsons SF, Lee G, Spring FA, et al. Lutheran blood group glycoprotein and its newly characterized mouse homologue specifically bind alpha5 chain-containing human laminin with high affinity. Blood 2001;97:312–20.
113. Odievre MH, Bony V, Benkerrou M, et al. Modulation of erythroid adhesion receptor expression by hydroxyurea in children with sickle cell disease. Haematologica 2008;93:502–10.
114. El Nemer W, Gane P, Colin Y, et al. The Lutheran blood group glycoproteins, the erythroid receptors for laminin, are adhesion molecules. J Biol Chem 1998;273:16686–93.
115. Wondimu Z, Gorfu G, Kawataki T, et al. Characterization of commercial laminin preparations from human placenta in comparison to recombinant laminins 2 (alpha2beta1gamma1), 8 (alpha4beta1gamma1), 10 (alpha5beta1gamma1). Matrix Biol 2006;25:89–93.
116. Champliaud MF, Virtanen I, Tiger CF, Korhonen M, Burgeson R, Gullberg D. Posttranslational modifications and beta/gamma chain associations of human laminin alpha1 and laminin alpha5 chains: purification of laminin-3 from placenta. Exp Cell Res 2000;259:326–35.
117. Zamurs L, Pouliot N, Gibson P, Hocking G, Nice E. Strategies for the purification of laminin-10 for studies on colon cancer metastasis. Biomed Chromatogr 2003;17:201–11.
118. Cines DB, Pollak ES, Buck CA, et al. Endothelial cells in physiology and in the pathophysiology of vascular disorders. Blood 1998;91:3527–61.
119. Mohandas N, Evans E. Adherence of sickle erythrocytes to vascular endothelial cells: requirement for both cell membrane changes and plasma factors. Blood 1984;64:282–7.
120. Mohandas N, Evans E. Sickle erythrocyte adherence to vascular endothelium. Morphologic correlates and the requirement for divalent cations and collagen-binding plasma proteins. J Clin Invest 1985;76:1605–12.
121. Turgeon ML. Clinical hematology: theory and procedures. 4th ed. Baltimore, MD: Lippincott Williams & Wilkins, 2004.
122. Akinsheye I, Alsultan A, Solovieff N, et al. Fetal hemoglobin in sickle cell anemia. Blood 2011;118:19–27.
123. Kato GJ, McGowan V, Machado RF, et al. Lactate dehydrogenase as a biomarker of hemolysis-associated nitric oxide resistance, priapism, leg ulceration, pulmonary hypertension, and death in patients with sickle cell disease. Blood 2006;107:2279–85.
124. Steinberg MH. Predicting clinical severity in sickle cell anaemia. Br J Haematol 2005;129:465–81.
125. Matsui NM, Borsig L, Rosen SD, Yaghmai M, Varki A, Embury SH. P-selectin mediates the adhesion of sickle erythrocytes to the endothelium. Blood 2001;98:1955–62.
126. Bartolucci P, Chaar V, Picot J, et al. Decreased sickle red blood cell adhesion to laminin by hydroxyurea is associated with inhibition of Lu/BCAM protein phosphorylation. Blood 2010;116:2152–9.
127. Smith BD, La Celle PL. Erythrocyte-endothelial cell adherence in sickle cell disorders. Blood 1986;68:1050–4.
128. Hebbel RP, Yamada O, Moldow CF, Jacob HS, White JG, Eaton JW. Abnormal adherence of sickle erythrocytes to cultured vascular endothelium: possible mechanism for microvascular occlusion in sickle cell disease. J Clin Invest 1980;65:154–60.
129. Gambero S, Canalli AA, Traina F, et al. Therapy with hydroxyurea is associated with reduced adhesion molecule gene and protein expression in sickle red cells with a concomitant reduction in adhesive properties. Eur J Haematol 2007;78:144–51.
130. Belcher JD, Chen C, Nguyen J, et al. Heme triggers TLR4 signaling leading to endothelial cell activation and vaso-occlusion in murine sickle cell disease. Blood 2014;123:377–90.
131. Chen G, Zhang D, Fuchs TA, Manwani D, Wagner DD, Frenette PS. Heme-induced neutrophil extracellular traps

contribute to the pathogenesis of sickle cell disease. Blood 2014; 123:3818–27.
132. Gladwin MT, Schechter AN, Ognibene FP, et al. Divergent nitric oxide bioavailability in men and women with sickle cell disease. Circulation 2003;107:271–8.
133. Jison ML, Gladwin MT. Hemolytic anemia-associated pulmonary hypertension of sickle cell disease and the nitric oxide/arginine pathway. Am J Respir Crit Care Med 2003; 168:3–4.
134. Reiter CD, Wang X, Tanus-Santos JE, et al. Cell-free hemoglobin limits nitric oxide bioavailability in sickle-cell disease. Nat Med 2002;8:1383–9.
135. Rother RP, Bell L, Hillmen P, Gladwin MT. The clinical sequelae of intravascular hemolysis and extracellular plasma hemoglobin: a novel mechanism of human disease. JAMA 2005;293: 1653–62.
136. Bensinger TA, Gillette PN. Hemolysis in sickle cell disease. Arch Intern Med 1974;133:624–31.
137. McCurdy PR, Sherman AS. Irreversibly sickled cells and red cell survival in sickle cell anemia: a study with both DF32P and 51CR. Am J Med 1978;64:253–8.
138. Kato GJ, Gladwin MT, Steinberg MH. Deconstructing sickle cell disease: reappraisal of the role of hemolysis in the development of clinical subphenotypes. Blood Rev 2007;21:37–47.
139. Chen J, Hobbs WE, Le J, Lenting PJ, de Groot PG, Lopez JA. The rate of hemolysis in sickle cell disease correlates with the quantity of active von Willebrand factor in the plasma. Blood 2011;117:3680–3.
140. Rakotoson MG, Di Liberto G, Audureau E, et al. Biological parameters predictive of percent dense red blood cell decrease under hydroxyurea. Orphanet J Rare Dis 2015;10:57.
141. Adegbola M. Genomics and pain research in sickle cell disease: an explanation of heterogeneity? ISRN Nursing 2011;2011: 672579.
142. Adegbola MA. Can heterogeneity of chronic sickle-cell disease pain be explained by genomics? A literature review. Biological Research for Nursing 2009;11:81–97.
143. Siller-Matula JM, Merhi Y, Tanguay JF, et al. ARC15105 is a potent antagonist of von Willebrand factor mediated platelet activation and adhesion. Arterioscler Thromb Vasc Biol 2012; 32:902–9.
144. Nimjee SM, Lohrmann JD, Wang H, et al. Rapidly regulating platelet activity in vivo with an antidote controlled platelet inhibitor. Mol Ther 2012;20:391–7.
145. Rowe JA, Claessens A, Corrigan RA, Arman M. Adhesion of plasmodium falciparum-infected erythrocytes to human cells: molecular mechanisms and therapeutic implications. Expert Reviews in Molecular Medicine 2009;11:e16.
146. Lu J, Fan T, Zhao Q, et al. Isolation of circulating epithelial and tumor progenitor cells with an invasive phenotype from breast cancer patients. Int J Cancer 2010;126:669–83.
147. Eriksson AC, Jonasson L, Lindahl TL, Hedback B, Whiss PA. Static platelet adhesion, flow cytometry and serum TXB2 levels for monitoring platelet inhibiting treatment with ASA and clopidogrel in coronary artery disease: a randomised cross-over study. Journal of Translational Medicine 2009;7:42.
148. Hines PC, Krishnamoorthy S, White J, et al. Natalizumab Blocks VLA-4 mediated red blood cell adhesion and is a potential therapy for sickle cell disease. Blood 2014;124:221.
149. Zennadi R, Hines PC, De Castro LM, Cartron JP, Parise LV, Telen MJ. Epinephrine acts through erythroid signaling pathways to activate sickle cell adhesion to endothelium via LW-alphavbeta3 interactions. Blood 2004;104:3774–81.
150. Delahunty M, Zennadi R, Telen MJ. LW protein: a promiscuous integrin receptor activated by adrenergic signaling. Transfus Clin Biol 2006;13:44–9.
151. Telen MJ. Erythrocyte adhesion receptors: blood group antigens and related molecules. Transfus Med Rev 2005;19:32–44.
152. Zennadi R, Moeller BJ, Whalen EJ, et al. Epinephrine-induced activation of LW-mediated sickle cell adhesion and vaso-occlusion in vivo. Blood 2007;110:2708–17.
153. De Castro LM, Zennadi R, Jonassaint JC, Batchvarova M, Telen MJ. Effect of propranolol as antiadhesive therapy in sickle cell disease. Clinical and Translational Science 2012; 5:437–44.
154. Finnegan EM, Barabino GA, Liu XD, Chang HY, Jonczyk A, Kaul DK. Small-molecule cyclic alpha V beta 3 antagonists inhibit sickle red cell adhesion to vascular endothelium and vaso-occlusion. Am J Physiol Heart Circ Physiol 2007;293: H1038–45.
155. Matsui NM, Varki A, Embury SH. Heparin inhibits the flow adhesion of sickle red blood cells to P-selectin. Blood 2002; 100:3790–6.
156. Alshaiban A, Muralidharan-Chari V, Nepo A, Mousa SA. Modulation of sickle red blood cell adhesion and its associated changes in biomarkers by sulfated nonanticoagulant heparin derivative. Clin Appl Thromb Hemost 2016;22:230–8.
157. Kutlar A, Ataga KI, McMahon L, et al. A potent oral P-selectin blocking agent improves microcirculatory blood flow and a marker of endothelial cell injury in patients with sickle cell disease. Am J Hematol 2012;87:536–9.
158. Kutlar A, Embury SH. Cellular adhesion and the endothelium: P-selectin. Hematol Oncol Clin North Am 2014;28:323–39.
159. Telen MJ. Cellular adhesion and the endothelium: E-selectin, L-selectin, and pan-selectin inhibitors. Hematol Oncol Clin North Am 2014;28:341–54.
160. Field JJ, Nathan DG. Advances in sickle cell therapies in the hydroxyurea era. Mol Med 2014;20(Suppl 1):S37–42.
161. Okpala I. Investigational selectin-targeted therapy of sickle cell disease. Expert Opin Investig Drugs 2015;24:229–38.
162. Telen MJ, Wun T, McCavit TL, et al. Randomized phase 2 study of GMI-1070 in SCD: reduction in time to resolution of vaso-occlusive events and decreased opioid use. Blood 2015;125: 2656–64.
163. Hidalgo A, Chang J, Jang JE, Peired AJ, Chiang EY, Frenette PS. Heterotypic interactions enabled by polarized neutrophil microdomains mediate thromboinflammatory injury. Nat Med 2009; 15:384–91.
164. Chang J, Patton JT, Sarkar A, Ernst B, Magnani JL, Frenette PS. GMI-1070, a novel pan-selectin antagonist, reverses acute vascular occlusions in sickle cell mice. Blood 2010;116: 1779–86.
165. Manwani D, Chen G, Carullo V, et al. Single-dose intravenous gamma globulin can stabilize neutrophil Mac-1 activation in sickle cell pain crisis. Am J Hematol 2015;90:381–5.
166. Turhan A, Weiss LA, Mohandas N, Coller BS, Frenette PS. Primary role for adherent leukocytes in sickle cell vascular occlusion: a new paradigm. Proc Natl Acad Sci U S A 2002;99: 3047–51.
167. Belcher JD, Marker PH, Weber JP, Hebbel RP, Vercellotti GM. Activated monocytes in sickle cell disease: potential role in the activation of vascular endothelium and vaso-occlusion. Blood 2000;96:2451–9.
168. Shet AS, Aras O, Gupta K, et al. Sickle blood contains tissue factor-positive microparticles derived from endothelial cells and monocytes. Blood 2003;102:2678–83.

169. Setty BN, Key NS, Rao AK, et al. Tissue factor-positive monocytes in children with sickle cell disease: correlation with biomarkers of haemolysis. Br J Haematol 2012;157:370–80.
170. Perelman N, Selvaraj SK, Batra S, et al. Placenta growth factor activates monocytes and correlates with sickle cell disease severity. Blood 2003;102:1506–14.
171. Kaul DK, Hebbel RP. Hypoxia/reoxygenation causes inflammatory response in transgenic sickle mice but not in normal mice. J Clin Invest 2000;106:411–20.
172. Hofstra TC, Kalra VK, Meiselman HJ, Coates TD. Sickle erythrocytes adhere to polymorphonuclear neutrophils and activate the neutrophil respiratory burst. Blood 1996;87:4440–7.
173. Chang J, Shi PA, Chiang EY, Frenette PS. Intravenous immunoglobulins reverse acute vaso-occlusive crises in sickle cell mice through rapid inhibition of neutrophil adhesion. Blood 2008; 111:915–23.
174. Miller ST, Sleeper LA, Pegelow CH, et al. Prediction of adverse outcomes in children with sickle cell disease. N Engl J Med 2000;342:83–9.
175. Wongtong N, Jones S, Deng Y, Cai J, Ataga KI. Monocytosis is associated with hemolysis in sickle cell disease. Hematology 2015;20:593–7.
176. Elmariah H, Garrett ME, De Castro LM, et al. Factors associated with survival in a contemporary adult sickle cell disease cohort. Am J Hematol 2014;89:530–5.
177. Field JJ, Nathan DG, Linden J. Targeting iNKT cells for the treatment of sickle cell disease. Clin Immunol 2011;140:177–83.
178. Field JJ, Lin G, Okam MM, et al. Sickle cell vaso-occlusion causes activation of iNKT cells that is decreased by the adenosine A2A receptor agonist regadenoson. Blood 2013;121:3329–34.
179. Ataga KI, Orringer EP. Hypercoagulability in sickle cell disease: a curious paradox. Am J Med 2003;115:721–8.
180. Frenette PS. Sickle cell vaso-occlusion: multistep and multicellular paradigm. Curr Opin Hematol 2002;9:101–6.
181. Barabino GA, Wise RJ, Woodbury VA, et al. Inhibition of sickle erythrocyte adhesion to immobilized thrombospondin by von Willebrand factor under dynamic flow conditions. Blood 1997; 89:2560–7.
182. Wick TM, Moake JL, Udden MM, McIntire LV. Unusually large von Willebrand factor multimers preferentially promote young sickle and nonsickle erythrocyte adhesion to endothelial cells. Am J Hematol 1993;42:284–92.
183. Kaul DK, Nagel RL. Sickle cell vasoocclusion: many issues and some answers. Experientia 1993;49:5–15.
184. Mohandas N, Evans E. Rheological and adherence properties of sickle cells. Potential contribution to hematologic manifestations of the disease. Ann N Y Acad Sci 1989;565:327–37.
185. Wick TM, Moake JL, Udden MM, Eskin SG, Sears DA, McIntire LV. Unusually large von Willebrand factor multimers increase adhesion of sickle erythrocytes to human endothelial cells under controlled flow. J Clin Invest 1987; 80:905–10.
186. Hebbel RP, Visser MR, Goodman JL, Jacob HS, Vercellotti GM. Potentiated adherence of sickle erythrocytes to endothelium infected by virus. J Clin Invest 1987;80:1503–6.
187. Hebbel RP, Boogaerts MA, Eaton JW, Steinberg MH. Erythrocyte adherence to endothelium in sickle-cell anemia. N Engl J Med 1980;302:992–5.
188. Whelihan MF, Mooberry MJ, Zachary V, et al. The contribution of red blood cells to thrombin generation in sickle cell disease: meizothrombin generation on sickled red blood cells. J Thromb Haemost 2013;11:2187–9.
189. Lim MY, Ataga KI, Key NS. Hemostatic abnormalities in sickle cell disease. Curr Opin Hematol 2013;20:472–7.

Appendix

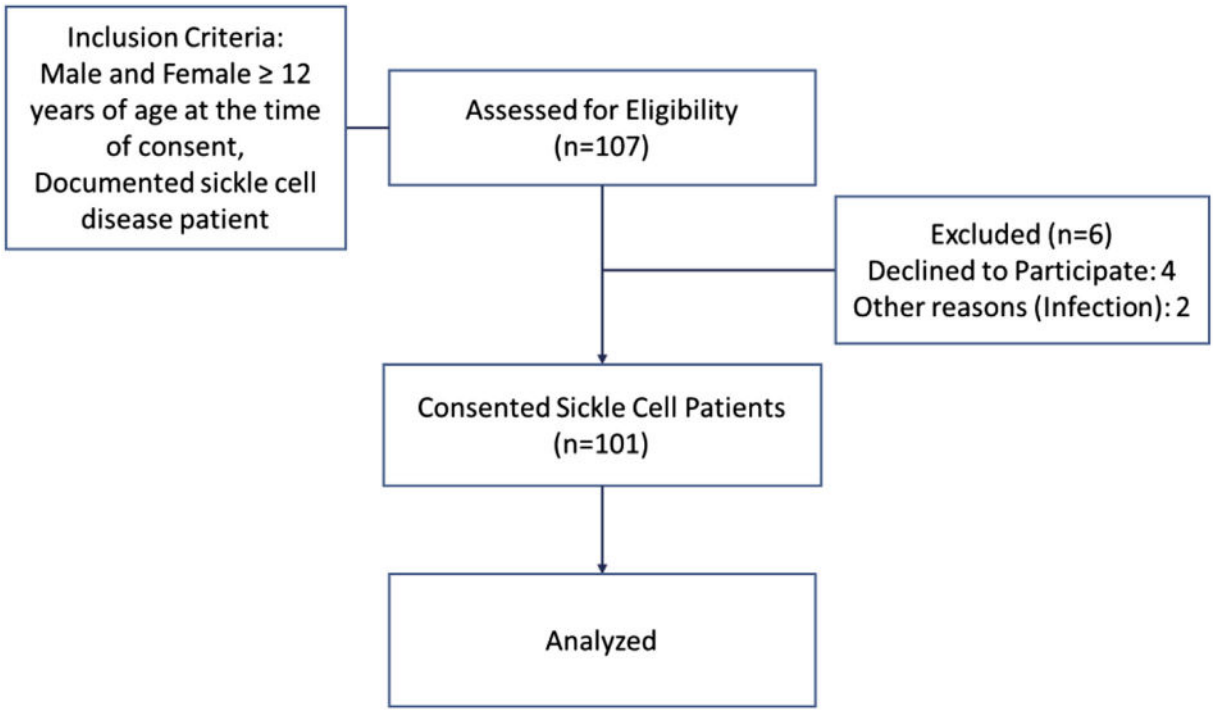

Fig S1. Consort-type diagram showing inclusion and exclusion criteria for subject recruitment.

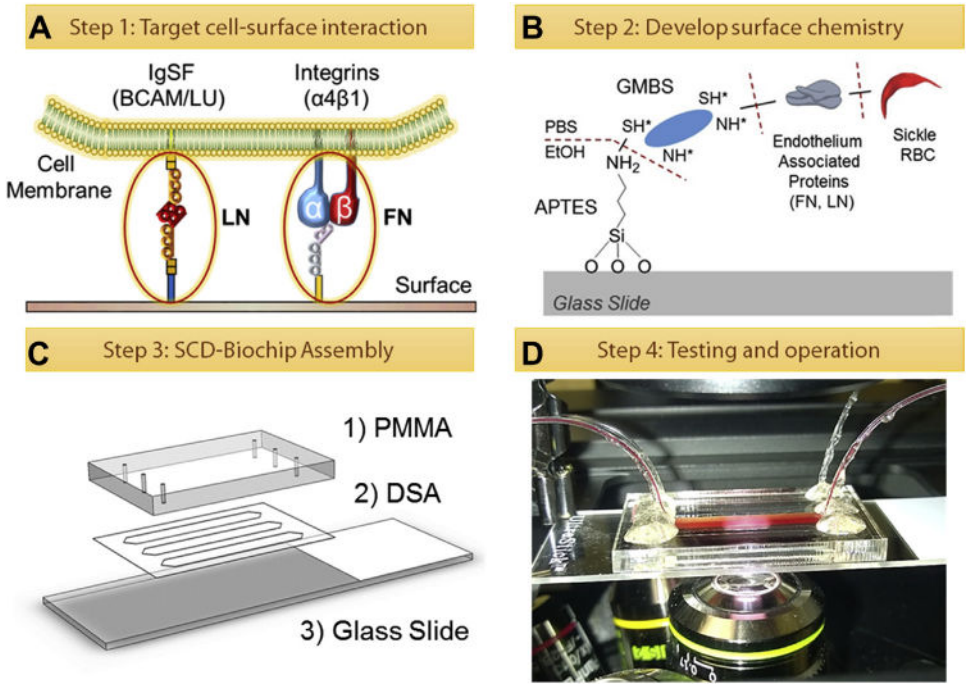

Fig S2. Development and fabrication of SCD biochip. (**A**) Adhesion receptors from the immunoglobulin superfamily (IgSF) BCAM/LU and integrin family ($\alpha 4\beta 1$) are targeted for adhesion to endothelial and subendothelial associated proteins, FN and LN. (**B**) FN and LN are covalently tethered to the glass slide through a cross linker (GMBS) and a self-assembled silane monolayer coating (APTES). (**C**) Assembly of the SCD biochip, composed of a polymethyl methacrylate (PMMA) cover, with micromachined inlets and outlets, a double-sided adhesive (DSA) layer, which defines the channel shape and height, and a glass slide base. (**D**) SCD biochip placed on a microscope stage for live cell imaging.

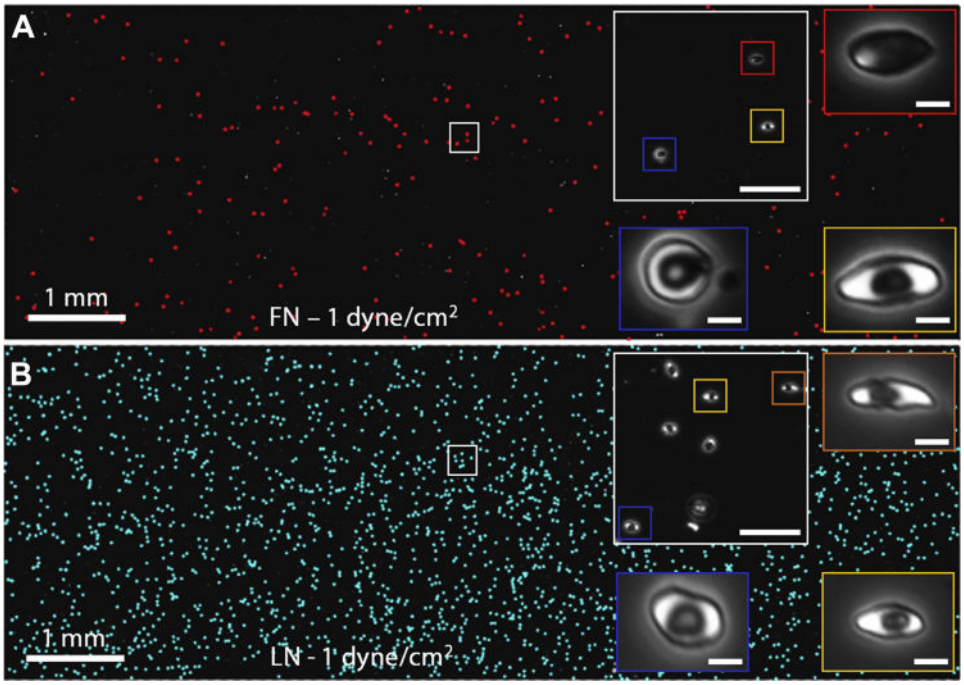

Fig S3. Close-up view of FN- and LN-adhered HbSS RBCs. (**A** and **B**) RBC adhesion was quantified using high resolution images of whole microchannels. Typical morphologies of adhered RBCs from HbSS blood samples in (**A**) FN- and (**B**) LN-functionalized microchannels are shown in subsequent insets. Scale bar represents 50 and 5 μm length, respectively.

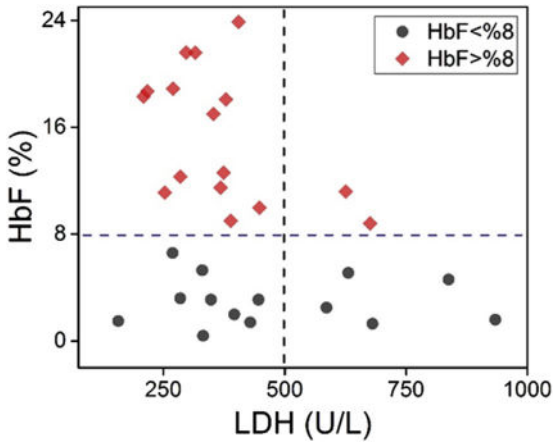

Fig S4. Serum LDH levels of SCD subjects with respect to corresponding percent (%) HbF.

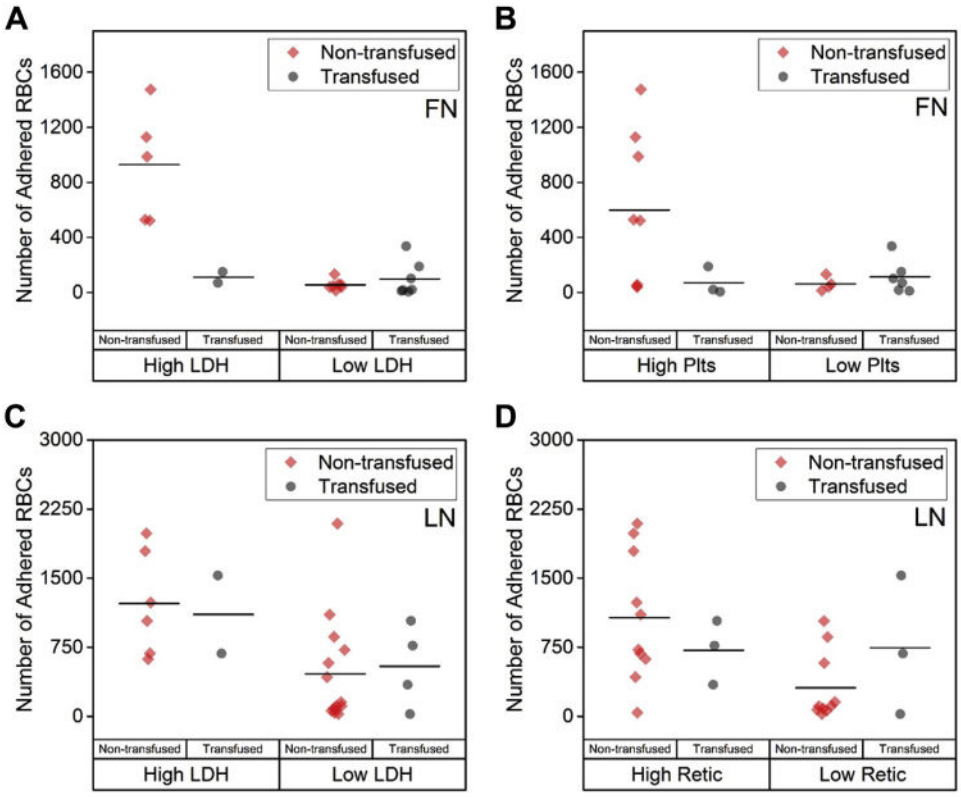

Fig S5. Adhesion of RBCs in transfused and nontransfused blood samples with high and low LDH levels, platelet counts, and reticulocyte counts. (**A** and **B**) RBCs in transfused blood samples with either high or low LDH and platelet counts (Plts) displayed low adherence to FN. (**C** and **D**) RBC adherence to LN was comparable in transfused and nontransfused blood samples with either high or low LDH and low reticulocyte counts.

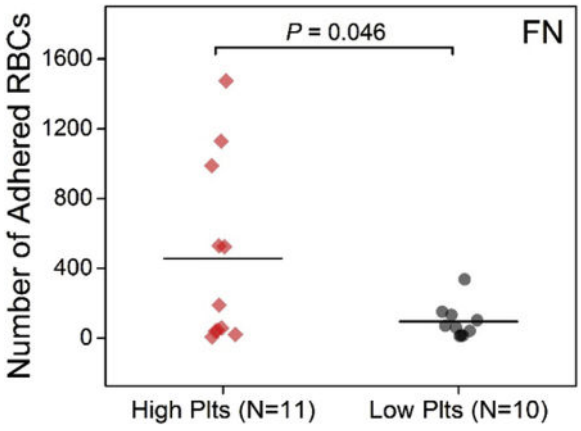

Fig S6. RBC adhesoneion to FN is associated with platelet counts in HbSS patients. Number of adhered RBCs in FN microchannels was significantly higher in blood samples with high platelet counts (Plts, $>320\ 10^9$/L). The horizontal lines between individual groups represent a statistically significant difference based on one-way ANOVA test ($P < 0.05$). Data point cross bars represent the mean. "N" represents the number of subjects.

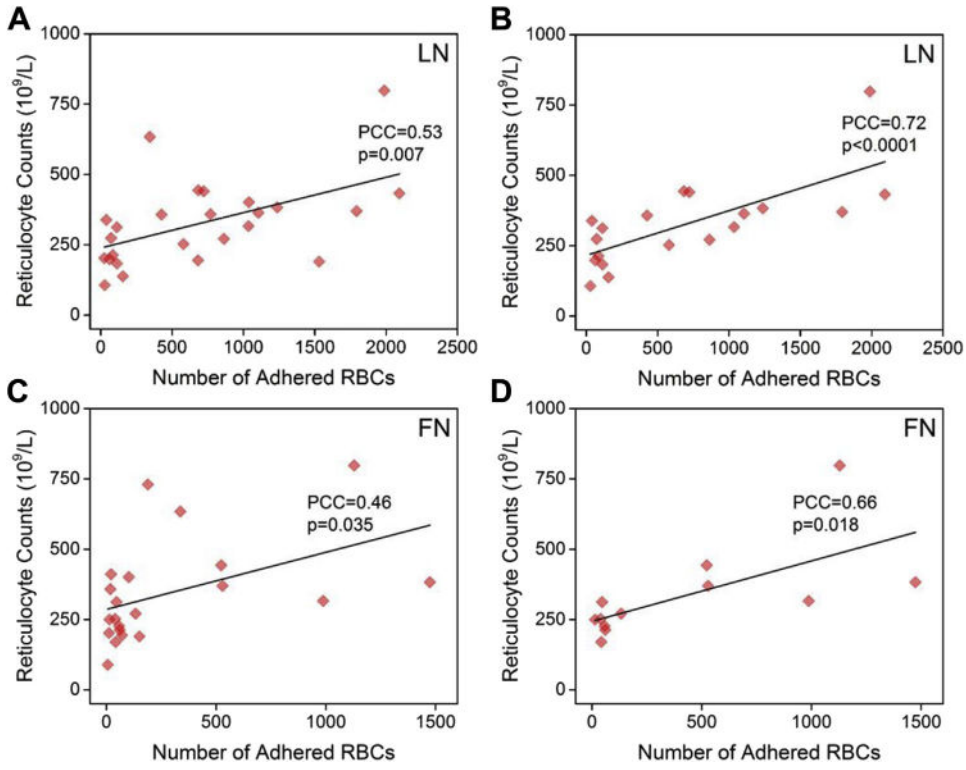

Fig S7. Correlation of RBC adhesion to FN and LN, and reticulocyte counts in (**A** and **C**), all studied SCD subjects, and in (**B** and **D**) nontransfused SCD subjects. Correlation between number of adhered RBCs and reticulocyte counts increased when transfused subjects were excluded.

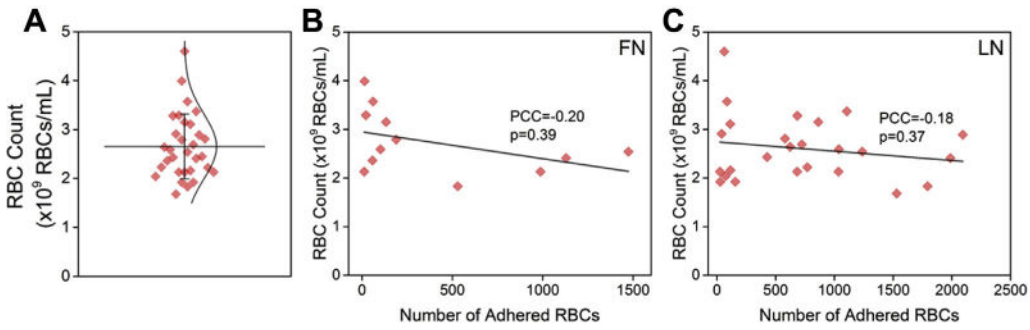

Fig S8. RBC counts in analyzed SCD patient whole blood samples and correlation with RBC adhesion to FN and LN. (**A**) RBC counts showed an average of $2.65 \pm 0.66 \times 10^9$ RBCs/mL (mean $\pm$ SD), where 21 of 31 blood samples had RBC counts within $1.9–2.9 \times 10^9$ RBCs/mL. (**B** and **C**) There was no statistically significant correlation between RBC counts of the blood samples and number of adhered RBCs to FN and LN.

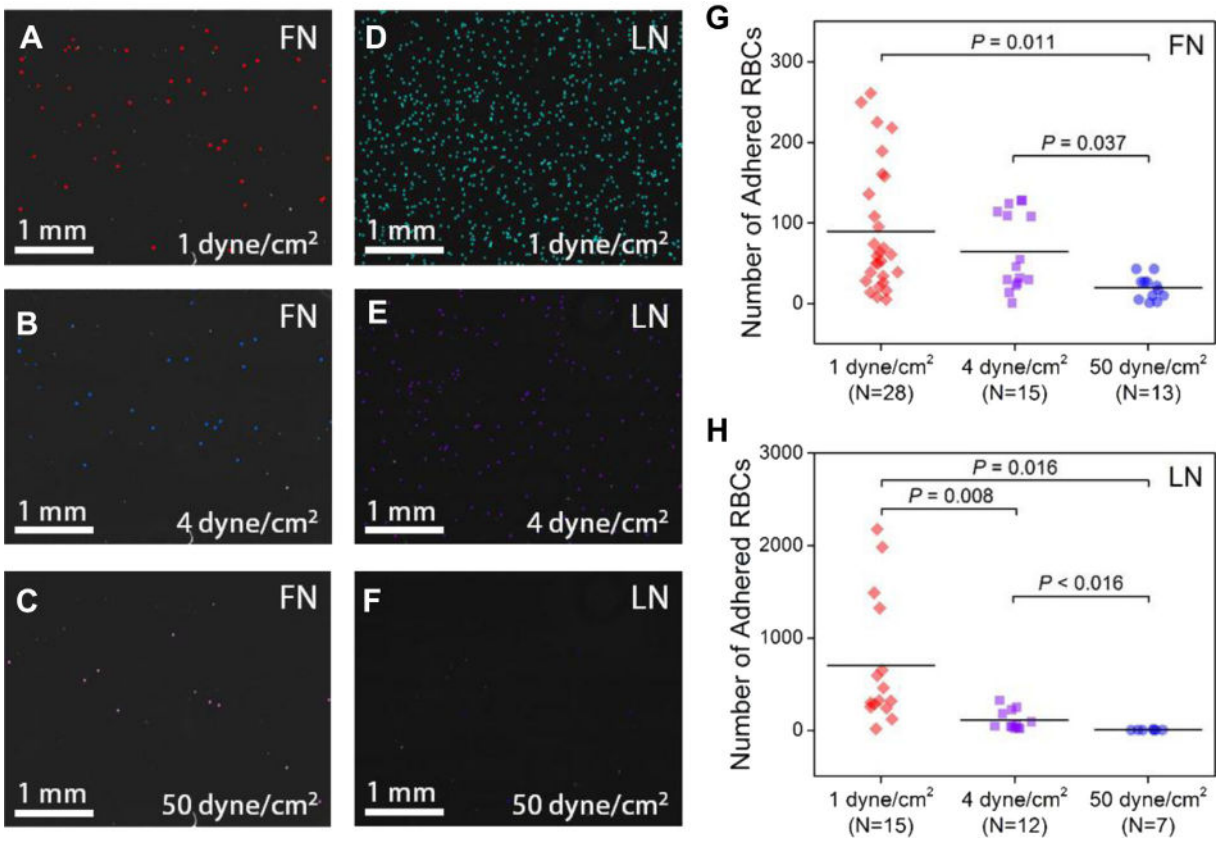

Fig S9. RBC adhesion to FN- and LN-functionalized microchannels in HbSS blood samples at different flow velocities. Microchannel images show RBC adhesion in (**A**–**C**) FN- and (**D**–**F**) LN-immobilized microchannels at (**A** and **D**) 1 dyne/cm^2, (**B** and **E**) 4 dyne/cm^2, and (**C** and **F**) 50 dyne/cm^2 flow shear stresses. (**G** and **H**) Shown is quantitation of adhered RBCs, at 50 dyne/cm^2 shear stress compared with 1 dyne/cm^2 and 4 dyne/cm^2 shear stress to FN- (**G**) and LN-immobilized (**H**) microchannels. The horizontal lines between individual groups represent a statistically significant difference based on a one-way ANOVA test ($P < 0.05$). Data point cross bars represent the mean. "N" represents the number of subjects.

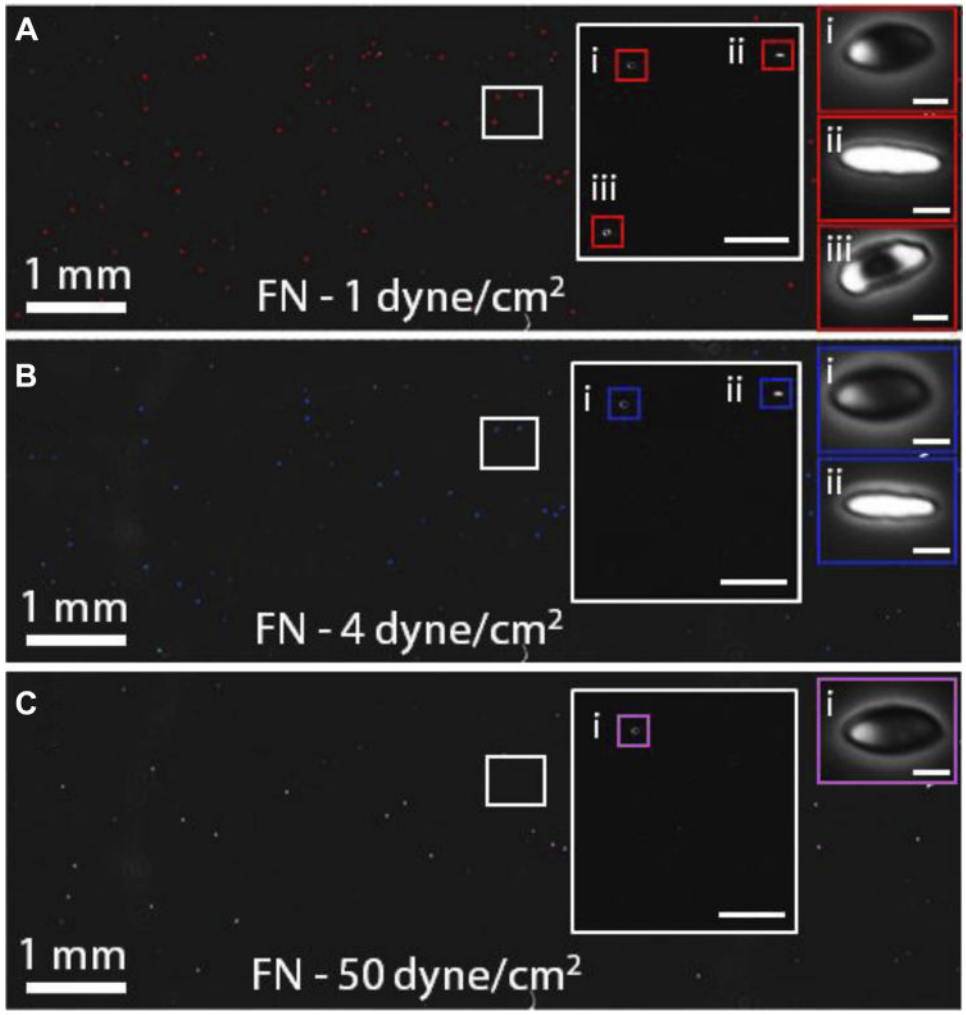

Fig S10. Close-up view of RBCs adhered to FN-immobilized microchannels in HbSS blood samples under precisely controlled flow velocities. (**A–C**) Microchannel images showed RBC adhesion in FN-immobilized microchannels and typical cell morphologies at (**A**) 1 dyne/cm^2, (**B**) 4 dyne/cm^2, and (**C**) 50 dyne/cm^2 flow shear stresses. RBCs with characteristic biconcave shape along with RBCs lacking biconcave morphology were noted in FN microchannels. Scale bar represents 50 and 5 μm length, respectively.

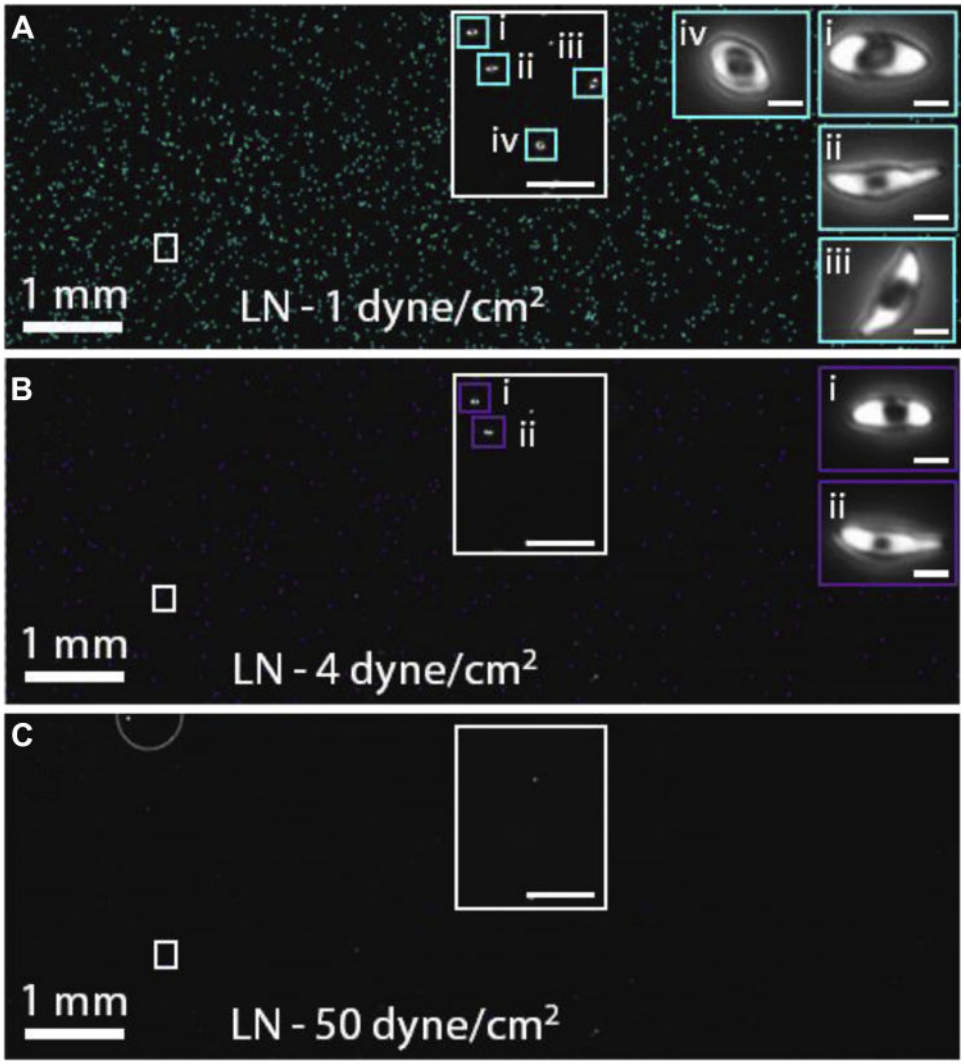

Fig S11. Close-up view of RBCs adhered to LN-immobilized microchannels in HbSS blood samples under precisely controlled flow velocities. (**A**–**C**) Microchannel images showed RBC adhesion in FN-immobilized microchannels and typical cell morphologies at (**A**) 1, (**B**) 4, and (**C**) 50 dyne/cm^2 flow shear stresses. Only RBCs with characteristic biconcave shape were observed in LN microchannels. Scale bar represents 50 and 5 μm length, respectively.

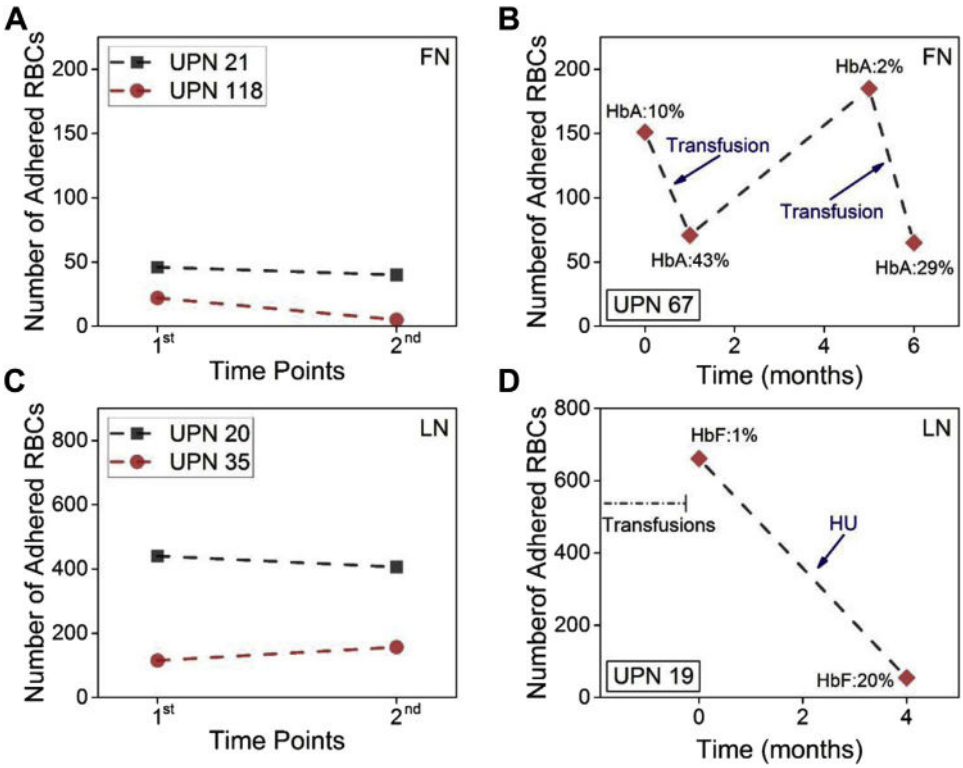

Fig S12. Cellular adhesion reflects clinical status in SCD. Shown are longitudinal analyses of adhesion to (**A**) FN. In UPN 118, stably transfused at 38%–42% HbA, and analyzed 1 month apart; in UPN 21, on hydroxyurea with a stable HbF (18%–19%), analyzed 4 months apart. (**B**) FN. In UPN 67, after transfusions, analyzed at 0, 1, 5, and 6 months. (**C**) LN. In UPN 20, managed with supportive care only and analyzed 2 months apart, and in UPN 35, managed with hydroxyurea (HbF, 22%–25%), analyzed 9 months apart. (**D**) LN. In UPN 19, over 4 months, after initiation of hydroxyurea therapy. (UPN: unique patient number).